Accepted Manuscript

Diphenylpyrroles: Novel p53 Activators

Sobhi M. Gomha , Taha M.A. Eldebss , Mohamed M. Abdulla , Abdelrahman S. Mayhoub

PII: S0223-5234(14)00514-5

DOI: 10.1016/j.ejmech.2014.05.082

Reference: EJMECH 7040

To appear in: *European Journal of Medicinal Chemistry*

Received Date: 17 May 2014

Revised Date: 23 May 2014

Accepted Date: 31 May 2014

Please cite this article as: S.M. Gomha, T.M.A. Eldebss, M.M. Abdulla, A.S. Mayhoub, Diphenylpyrroles: Novel p53 Activators, *European Journal of Medicinal Chemistry* (2014), doi: 10.1016/j.ejmech.2014.05.082.

- Blocking p53 binding site on HDM2 was believed to generate efficient antitumor agents
- Diphenylpyrroles were introduced and evaluated as a novel scaffold in the field of p53 activators
- New 4,5-diphenyl-3-heteroaryl-pyrroles were synthesized *via* reactions of enaminones with C- and N-nucleophiles.
- Diphenylpyrroles scaffold has the advantage of synthetic protocol accessibility

Graphical Abstract

Diphenylpyrroles: Novel p53 Activators

Sobhi M. Gomha[a*], Taha M. A. Eldebss,[a] Mohamed M. Abdulla[b] and Abdelrahman S. Mayhoub[c]

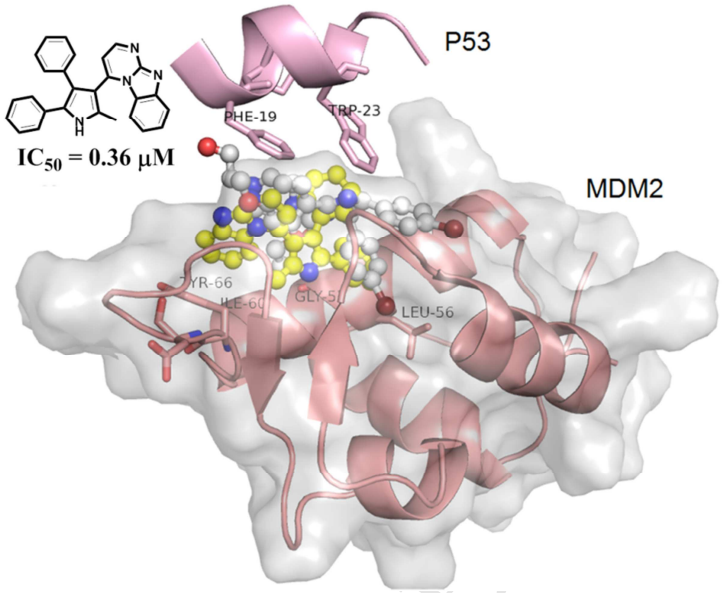

An efficient synthesis of novel 4,5-diphenyl-3-heteroaryl-pyrroles were synthesized and evaluated as a novel scaffold in the field of p53 activators.

Diphenylpyrroles: Novel p53 Activators

Sobhi M. Gomha[a*], Taha M. A. Eldebss,[a] Mohamed M. Abdulla[b] and Abdelrahman S. Mayhoub[c]

[a]*Department of Chemistry, Faculty of Science, Cairo University, Giza 12613, Egypt*
[b]*Research Unit, Saco Pharm. Co., 6th October City, Egypt*
[c]*Department of Organic Chemistry, Faculty of Pharmacy, Al-Azhar University, Cairo, 11884 Egypt*

Abstract: Cellular tumor antigen p53 is crucial for cancer prevention via different mechanisms. E3 ubiquitin-protein ligase HDM2 binds to p53, blocks its ability to activate transcription, and therefore acts as a negative regulator. Blocking p53 binding site on HDM2 was believed to generate efficient antitumor agents. So far, limited scaffolds were reported with HDM2 antagonist activity. Herein, diphenylpyrroles were introduced and evaluated as a novel scaffold in the field of p53 activators. An efficient synthesis of novel 3-heteroaryl-pyrroles is described *via* reactions of *E*-3-(dimethylamino)-1-(2-methyl-4,5-diphenyl-1*H*-pyrrol-3-yl)prop-2-en-1-one or *E*-1-(2-methyl-4,5-diphenyl-1*H*-pyrrol-3-yl)-3-morpholinoprop-2-en-1-one with hydrazine hydrate, phenyl hydrazine, hydroxylamine, various heterocyclic amines and active methylene compounds.

Keywords: Pyrroles, triazolopyrimidine, benzimidazopyrimidine, pyrazolopyrimidine, and p53-specific ubiquitin E3 ligase HDM2.

1. Introduction

The tumor suppressor protein p53 is central to mammalian cells protection mechanism against malignant transformation. So far, p53 is inactivated in a large proportion of cancer cells [1]. p53 is regulated by another protein called human double minute 2 (HDM2). HDM2 binds to p53 at its transactivating domain and block its ability to activate transcription. Therefore, it acts as a negative regulator to p53 suppressor protein [2, 3]. Moreover, the oncogene HDM2 and p53 are linked in a negative feed-back loop in which p53 activates HDM2 [4]. HDM2 is acting as a p53-specific ubiquitin E3 ligase and thus promoting degradation of p53 protein through the ubiquitin-proteosome system [5]. In the same vein, overexpression of p53 negative regulator HDM2 was observed in many human malignancies [6-15].

*Corresponding author, Tel: + 20100 1649576, Fax: + (202) 35727556
E-mail: s.m.gomha@hotmail.com

Recently, medicinal chemist adopted a strategy for the reactivation of the pro-apoptotic p53 activities, where HDM2 is overexpressed, is therefore to interrupt the p53-HDM2 feed-back loop, either by blocking the protein–protein interaction between the p53 N-terminal domain and HDM2, or by inhibiting the E3 ligase activity of HDM2 [16]. Several small molecules have been so far reported as p53-pathway modulators [17].The capability of 5-deazaflavin derivatives to activate the tumor suppressor p53 in cancer cells was reported through inhibition of the p53-specific ubiquitin E3 ligase HDM2 (Chart 1) [18-20]. In addition, some diphenylimidazolidines, glucocorticoids and engineered cyclotides have been reported to play the same role [21, 22].

Chart 1. Chemical structures of some reported HDM2 ligase inhibitors.

Research Design: Aiming to expand the reported tumor suppressor p53 activators, we are reporting herein 2,3-diphenylpyrrole as a novel scaffold in the field of interrupting p53-HDM2 signaling pathway. Diphenylimidazolidine derivatives (Chart 1), reported by L. T. Vassilev, ranked among the most reported potent p53 activators [23]. The structures of all reported diphenylimidazolidines were built using Sybyl-X, aligned and a pharmacophore model was generated using Discovery Studio 3.1 as briefly shown in Chart 2 (ring substitutions and side chains were ignored at this stage). With this model in hand, a library of mono- and diphenyl-substituted 5-memebered compounds was virtually screened and the top scored structures were assayed for their p53-activation properties. These efforts collectively afforded compound **7** (Chart 2) that has a closely related pharmacophore (Chart 2).

Chart 2. Work Design

Chart 3. Alignment of reported (black) and newly (red) derived structures: The diphenyl rings of the lead structure (black) were reported to interact with MDM2 (PDB: 1rv1), leaving the other two groups facing p53.

The two phenyl rings of the lead diphenylimidazolidine were reported to interact with MDM2 protein, while the substituents at imidazolidine 2 and 3 positions were reported to interrelate with p53 [23]. Since diphenyl moieties of lead and newly presented structures are well-aligned together as shown in Chart 3, they are intuitively expected to bind similarly keeping the aromatic system at pyrrole-3 position facing the binding HDM2-pocket at p53. Our focus in this report was directed

towards modifying the aromatic system at pyrrole-3 position to comprehensively cover the structure-activity-relationships of this diphenylpyrrole as a new p53 activator.

2. Results and discussion

2.1. Chemistry

The starting *E*-3-(dimethylamino)-1-(2-methyl-4,5-diphenyl-1*H*-pyrrol-3-yl)prop-2-en-1-one (**3**) was prepared as previously described [24] *via* condensation of the pyrazole derivative **1** [25] with dimethylformamide dimethyl acetal (DMF-DMA, **2**). Treatment of the enaminone **3** with morpholine under reflux condition afforded enaminone **4** as shown in Scheme 1.

Scheme 1: Synthesis of compounds **3-5**

Treatment of **3** or **4** with *N*-nucleophile such as hydrazine hydrate and phenyl hydrazine in absolute ethanol under reflux gave 5-(2-methyl-4,5-diphenyl-1*H*-pyrrol-3-yl)-1*H*-pyrazole (**6**) and 5-(2-methyl-4,5-diphenyl-1*H*-pyrrol-3-yl)-1-phenyl-1*H*-pyrazole (**7**), respectively (Scheme 2) [26, 27]. Similar treatment of **3** or **4** with hydroxylamine hydrochloride in heated ethanol in the presence of potassium carbonate afforded only one isolable product that was identified, on the basis of its spectral and elemental analyses, as the isoxazole derivative **4** (Scheme 2). The structures of the products **6**, **7** and **8** were confirmed by their spectral (MS, IR, ^{1}H- and ^{13}C NMR) and elemental analyses data (see Experimental section). For example, their IR spectra revealed the absence of the carbonyl group present in the spectrum of the enaminone **3** or **4**. The ^{1}H NMR spectrum of **6** showed two characteristic signals at δ 6.38 with *J value* of 7.2 Hz, and 7.67 with the same *J value* of the pyrazole ring protons. Structure **8** was assigned for the reaction products on the basis of the ^{1}H NMR spectral data in which a resonance for H-4 and H-5 of isoxazole appeared typically at δ 6.38 and 8.37ppm, respectively [28].

Compounds **6-8** were supported by the alternate chemical synthesis via the reaction of sodium salt of 3-acetyl-2-methyl-4,5-diphenyl-1*H*-pyrrole (**5**) with hydrazine hydrate, phenyl hydrazine, and hydroxylamine hydrochloride in ethanol containing few drops of acetic acid, respectively (Scheme 1).

Scheme 2: Synthesis of pyrazoles **6**, **7** and isoxazole **8**

The reactivity of the enaminone **3** or the morpholinyl derivative **4** towards some heterocyclic amines were also examined. Thus, reaction of **3** or **4** with 5-amino-1*H*-pyrazole-4-carbonitrile **9** in acetic acid under reflux yielded the respective pyrazolo[1,5-*a*]pyrimidine derivative **10** (Scheme 3). Similar treatment of **3** or **4** with 5-amino-1,2,4-triazole (**11**), 5-amino-1*H*-tetrazole (**13**), 2-aminobenzimidazole (**15**) and 6-amino-2-thioxo-2,3-dihydropyrimidin-4(1*H*)-one (**17**) under the same reaction conditions afforded the respective 1,2,4-triazolo[1,5-*a*]pyrimidine **12,** tetrazolo[1,5-*a*]pyrimidine **14**, benzimidazo[1,2-*a*]pyrimidine **16** and 2,3-dihydropyrido[2,3-d]pyrimidinone **18** derivatives, respectively (Scheme 3).

Scheme 3: Synthesis of fused pyrimidines **10**, **12**, **14**, **16** and **18**

Pyrimidine-containing derivatives **10**, **12**, **14**, **16** and **18** were prepared by allowing enaminone **3** or **4** to react with a set of amine-containing heterocycles. The reaction passed through two main steps: fist, Michael-type addition of the exocyclic amine followed by *in situ* tandem elimination of dimethylamine (Scheme 4). The ^{1}H NMR spectrum of each final isolated products; i.e. **10**, **12**, **14** and **16**, revealed two doublets in the aromatic regions δ 8.09- 8.16 and 8.59- 8.76 with *J value* around 4.5 Hz assignable to the two vicinal protons of the pyrimidine ring [29-31].

Scheme 4: Mechanism of synthesis of fused pyrimidines **10, 12, 14,** and **16**

Next, pyridinyl analogues were prepared via reactions of the enaminone **3** or **4** with *C*-nucleophile such as active methylene compounds. Thus, reaction of **3** or **4** with acetylacetone **19a**, ethyl acetoacetate **19b** and ethyl benzoylacetate **19c** in acetic acid/ammonium acetate yielded 2-(pyrrol-3-yl) pyridine derivatives **20a-c**, respectively (Scheme 5). As also depicted in Scheme 5, the formation of **20** seems to start with Michael addition of the active methylene **19** to the activated double bond of **3** followed by tandem elimination of dimethylamine and condensation with ammonia. The other possible isomeric structure **21** was discarded on the basis of spectral data. For example, the ^{1}H NMR spectrum of each products **20a-c** exhibited two doublet signals in the regions of δ 7.75-7.76 and 8.32-8.39 due to pyridine H-3 and H-4, respectively with J value around 8.2 Hz. The latter coupling constant value is

characteristic for ortho H-3 and H-4 pyridine coupling, and much higher than the values of H-2 and H-3 (J = 4-6 *Hz*) [32].

Scheme 5: Synthesis of pyridines **20a-c**

Reactions of **3** or **4** with malononitrile **22a** and ethyl cyanoacetate **22b** in the presence of sodium ethoxide afforded products **23a** and **23b**, respectively. The assignments of their structures were based on their spectral and elemental analyses data (see Experimental section). Furthermore, the structure of **23a** was confirmed by an alternative synthesis; i.e. by reaction of **3** with cyanoacetamide **24a** under the same reaction conditions (Scheme 6). As discussed before, the formation of **23** was suggested to start with Michael addition of the active methylene compound **22** to the activated double bond of **3** followed by tandem cyclization, elimination of dimethylamine and Dimroth type rearrangement of the formed pyran intermediate to give **23** as the end product **(**Scheme 6).

.

Scheme 6: Synthesis of pyridinones **23a,b**

2.2. Pharmacology

Synthesized compounds were assayed for inhibition of p53 ubiquitination by incubation with GST-tagged HDM2, immobilized on glutathione-Sepharose, p53, ubiquitin, as well as E1 and E2 (UbcH5B) ligases, in an assay buffer containing ATP as detailed in references [33, 34]. The reaction products were then resolved by SDS-PAGE and p53 ubiquitination, and were quantified by Western blotting using an anti-p53 antibody [35].

Tested compounds that pass the preliminary assay; i.e. compounds that showed some activity at concentrations below 100 µM were then subjected to determination of half-maximal inhibition concentration (IC_{50}) of p53 ubiquitination using essentially the same assay methodology, except that a fluorescently labelled form of ubiquitin was used. After completion of the ubiquitination reaction, excess fluorescent ubiquitin was removed from the immobilized p53-HDM2 complex by centrifugation, and incorporation of ubiquitin was measured by fluorescence spectroscopy (Table 1).

Table 1: IC_{50} of p53 ubiquitination of the newly synthesized compounds (*in vitro)*

.

Figure 3. Hypothetical binding mode of compound **16** (colored yellow) and the reference diphenylimidazoline compound (colored light gray) in MDM2 protein (PDB: 1t4f).

To rationalize the observed HMD2 inhibition results, chemical structures of all biologically-tested compounds were built using Sybyl-X, subjected to energy minimization and docked within p53-binding site on HDM2 (PDB: 1t4f). The calculated binding mode of the most potent derivative, compound **16**, was presented in Figure 3 (colored yellow) as a representative example together with the reported diphenylimidazolidine derivative as a reference (colored light grey). Briefly, there is great similarity between the binding modes of both as hypothesized earlier. In more details, there is complete overlap between phenyl ring at pyrole position-2 and the phenyl ring of imidazolidine at positon-5. So far, both phenyl rings was calculated to be docked with a lipophililc pocket close to Leu56. The terminal benzene ring of the fused aromatic system at pyrrole postion-3 was calculated to interact favorably with the phenyl ring of Tyr66 and the lipothilic side chain of Ile60 via face to face π-π interaction (Figure 3).

Our model sheds lights on how diphenylpyrroles interact with HDM2; however calculating the binding modes of our inhibitors while both proteins interacting with each other is beyond our computational facilities. The reference compound was found to occupy the pocket normally occupied by Phe19, Try23, and Leu26 of p53 [23]. Analogously, we are expecting same type of interactions in case of our newly designed ligands; i.e. the phenyl ring at pyrrole position-4, in addition to the aromatic system at positon-3 is expected to interact with such lipophilic residues.

Finally, by examining of the SAR at pyrrole postion-3, we came up with some conclusions. The benzo[4,5]imidazo[1,2-*a*]pyrimidine linked to pyrrole ring increases the activity more than the 2-thioxo-2,3-dihydropyrido[2,3-*d*]pyrimidin-4(1*H*)-one. The 2-thioxo-2,3-dihydropyrido[2,3-*d*] pyrimidin-4(1*H*)-one increases the activity more than the pyridine. The pyridinone provide more activity profile than the pyridine. The pyridine moiety give rise to higher activity than the tetrazolo[1,5-*a*]pyrimidine one. The tetrazolo[1,5-*a*]pyrimidine moiety give rise to higher activity than the pyrazolo[1,5-*a*] pyrimidine. For pyridine derivatives **23a**, **b:** the ester group provides more activity than the cyano group. For derivatives **20a-c**: the phenyl moiety gives higher activity than the methyl one and

the ester give higher activity than the acetyl one. Isoxazole moiety increases the activity more than the pyrazole one.

3. Conclusion

In the investigation described above, a 4,5-diphenyl-3-heteroaryl-pyrroles were introduced as a new class of p53 activators. The scaffold has the advantage of synthetic protocol accessibility. Briefly, target compounds were prepared *via* reactions of *E*-3-(dimethylamino)-1-(2-methyl-4,5-diphenyl-1*H*-pyrrol-3-yl)prop-2-en-1-one or *E*-1-(2-methyl-4,5-diphenyl-1*H*-pyrrol-3-yl)-3-morpholinoprop-2-en-1-one with C- and N-nucleophiles.

4. Experimental protocols

4.1. Chemistry

4.1.1. General

All melting points were measured on a Gallenkamp melting point apparatus. The infrared spectra were recorded in potassium bromide disks on a Pye Unicam SP 3300 and Shimadzu FT IR 8101 PC infrared spectrophotometers. The NMR spectra were recorded on a Varian Mercury VX-300 NMR spectrometer. ^{1}H (300 MHz) and ^{13}C NMR (75.46 MHz) were run in deuterated dimethylsulphoxide (DMSO-d_6). Chemical shifts were related to that of the solvent. Mass spectra were recorded on a Shimadzu GCMS-QP 1000 EX mass spectrometer at 70 e.V. Elemental analyses were carried out at the Microanalytical Center of Cairo University, Giza, Egypt.

4.1.2. **Reactions of enaminone 3 or 4 with hydrazines**. To a solution of the enaminone **3** or **4** (1 mmol) in EtOH (10 mL) was added hydrazine hydrate (1 mL) or phenylhydrazine (1 mL) and the mixture was heated under reflux for 2 h. The reaction mixture was acidified by HCl / ice mixture and the formed product was filtered and crystallized from EtOH to give the respective pyrazoles **6** and **7**.

4.1.2.1. 5-(2-Methyl-4,5-diphenyl-1H-pyrrol-3-yl)-1H-pyrazole (**6**). Yield 88%, mp 232 °C; IR (KBr) υ: 3398, 3214 (2NH) cm^{-1}; ^{1}H NMR (DMSO-d_6) δ: 1.73 (s, 3H, CH_3), 6.37 (d, 1H, pyrazole- H4), 7.10–7.26 (m, 10H, Ar-H), 7.67 (d, 1H, pyrazole-H5), 10.81 (br., s, 1H, NH, D_2O exchangeable), 11.16 (br., s, 1H, NH, D_2O exchangeable) ppm; MS *m/z* (%): 300 (M^++1, 77), 299 (M^+, 100), 210 (93), 176 (72),

100 (80), 77 (60). Anal. Calcd for $C_{20}H_{17}N_3$ (299.37): C, 80.24; H, 5.72; N, 14.04. Found: C, 80.24; H, 5.72; N, 14.04%.

4.1.2.2. 5-(2-Methyl-4,5-diphenyl-1H-pyrrol-3-yl)-1-phenyl-1H-pyrazole **(7)**: Yield 82%, mp 243-245 °C; IR (KBr) υ: 3306 (NH) cm^{-1}; ^{1}H NMR (DMSO-d_6) δ: 1.83 (s, 3H, CH_3), 6.71 (d, 1H, pyrazole H-4), 7.12–7.44 (m, 15H, Ar-H), 7.68 (d, 1H, pyrazole-H5), 11.35 (br., s, 1H, NH, D_2O exchangeable); ^{13}C NMR (DMSO-*d*6): δ 13.7 (CH_3), 109.3, 112.3, 117.8, 123.1, 125.7, 126.1, 126.3, 126.4, 126.5, 127.7, 128.0, 128.1, 128.3, 128.4, 129.0, 130.7, 136.2, 139.6, 145.9 (Ar-C) ppm; MS *m/z* (%): 375 (M^+, 55), 318 (52), 256 (57), 172 (48), 92 (85), 77 (100). Anal. Calcd for $C_{26}H_{21}N_3$ (375.47): C, 83.17; H, 5.64; N, 11.19. Found: C, 83.11; H, 5.48; N, 11.04%.

4.1.3. **Alternative synthesis of compound 6.** A solution of sodium (2-methyl-4,5-diphenyl-1*H*-pyrrol-3-yl)-3-oxoprop-1-en-1-olate (**5**) (0.650 g, 2 mmol) and hydrazine hydrate (1 mL) in acetic acid (10 mL) was refluxed for 2 hr. After completion of the reaction, the hot reaction mixture was cooled and the solid products collected by filtration and recrystallized from EtOH gave product **6** in 80% yield, which were identical in all aspects (m.p., mixed m.p. and spectra) with those obtained from reaction of enaminone **3** or **4** with hydrazine hydrate.

4.1.4. **Synthesis of 3-(2-methyl-4,5-diphenyl-1*H*-pyrrol-3-yl)isoxazole (8)** Hydroxylamine hydrochloride (0.07 g, 1 mmol) was added to a mixture of enaminone **3** or **4** (1 mmol) and anhydrous potassium carbonate (0.5 g) in absolute EtOH (20 mL). The mixture was heated under reflux for 5 h and poured onto water. The solid product was filtered and crystallized from ethanol to give compound **8** in 86% yield, mp: 228-230 °C; IR (KBr) υ: 3251 (NH) cm^{-1}; ^{1}H NMR (DMSO-d_6) δ: 1.82 (s, 3H, CH_3), 6.42(d, 1H, isoxazole- H4), 7.19-7.45 (m, 10H, Ar-H), 8.42 (d, 1H, isoxazole-H5), 11.66 (br., s, 1H, NH, D_2O exchangeable) ppm; MS *m/z* (%): 301 (M^++1, 78), 300 (M^+, 52), 271 (82), 154 (95), 77 (100). Anal. Calcd for $C_{20}H_{16}N_2O$ (300.35): C, 79.98; H, 5.37; N, 9.33. Found: C, 79.69; H, 5.32; N, 9.18%.

4.1.5. **Reactions of enaminone 3 or 4 with heterocyclic amines**.

General procedure: A mixture of enaminone **3** or **4** (5 mmol) and the appropriate 5-amino-1*H*-pyrazole-4-carbonitrile **9**, aminotriazole **11**, aminotetrazole **13**, 2-aminobenzimidazole 1**5**, or 6-amino-2-thioxo-2,3-dihydropyrimidin-4(1*H*)-one **17** (5 mmol) in acetic acid (20 mL) was refluxed for 6 h. The

reaction mixture was cooled and diluted with MeOH and the solid product was collected by filtration and recrystallized from the suitable solvent gave products **10**, **12**, **14**, **16** or **18**, respectively. The synthesized compounds together with their physical and spectral data are listed below.

4.1.5.1. 7-(2-Methyl-4,5-diphenyl-1H-pyrrol-3-yl)pyrazolo[1,5-a]pyrimidine-3-carbonitrile (**10**): Yield 76%, mp 262-264 °C; IR (KBr) υ: 3311 (NH), 2229 (CN) cm^{-1}; ^1H NMR (DMSO-d_6) δ: 1.83 (s, 3H, CH_3), 7.07-7.56 (m, 10H, Ar-H), 8.34(1H, d, pyrimidine-H4), 8.42(1H, s, pyrazole-H), 9.59(1H, d, pyrimidine-H6), 11.59 (br., s, 1H, NH, D_2O exchangeable) ppm; MS *m/z* (%): 375 (M^+, 52), 331 (97), 218 (100), 189 (94), 102 (92), 87 (94), 64 (100). Anal. Calcd for $C_{24}H_{17}N_5$ (375.43): C, 76.78; H, 4.56; N, 18.65. Found: C, 76.58; H, 4.66; N, 18.41%.

4.1.5.2. 7-(2-Methyl-4,5-diphenyl-1H-pyrrol-3-yl)-[1,2,4]triazolo[1,5-a]pyrimidine (**12**): Yield 78%, mp 303-305 °C; IR (KBr) υ: 3249 (NH) cm^{-1}; ^1H NMR (DMSO-d_6) δ: 1.83 (s, 3H, CH_3), 7.03–7.44 (m, 10H, Ar-H), 8.14(1H, d, pyrimidine-H), 8.59(1H, d, pyrimidine-H), 9.03(1H, s, triazole-H), 11.58 (br., s, 1H, NH, D_2O exchangeable); ^{13}C NMR (DMSO-*d*6): δ 13.0 (CH_3), 116.1, 117.5, 118.7, 122.0, 125.6, 126.0, 126.5, 126.8, 128.0, 128.2, 128.9, 129.6, 129.7, 130.7, 132.1, 135.1, 137.0, 144.3, 146.4 (Ar-C) ppm; MS *m/z* (%): 352 (M^++1, 49), 351 (M^+, 100), 260 (83), 218 (73), 189 (67), 77 (78). Anal. Calcd for $C_{22}H_{17}N_5$ (351.40): C, 75.19; H, 4.88; N, 19.93. Found: C, 75.10; H, 4.76; N, 19.76%.

4.1.5.3. 7-(2-Methyl-4,5-diphenyl-1H-pyrrol-3-yl)tetrazolo[1,5-a]pyrimidine (**14**): Yield 76%, mp 256-257 °C; IR (KBr) υ: 3266 (NH) cm^{-1}; ^1H NMR (DMSO-d_6) δ: 1.75 (s, 3H, CH_3), 7.12–7.37 (m, 10H, Ar-H), 8.14(1H, d, pyrimidine-H), 8.52(1H, d, pyrimidine-H), 11.59 (br., s, 1H, NH, D_2O exchangeable) ppm; MS *m/z* (%): 353 (M^++1, 68), 352 (M^+, 100), 264 (86), 244 (86), 203 (89), 129 (79), 77 (76). Anal. Calcd for $C_{21}H_{16}N_6$ (352.39): C, 71.58; H, 4.58; N, 23.85. Found: C, 71.62; H, 4.51; N, 23.62%.

4.1.5.4. 4-(2-Methyl-4,5-diphenyl-1H-pyrrol-3-yl)benzo[4,5]imidazo[1,2-a]pyrimidine (**16**): Yield 76%, mp 256-257 °C; IR (KBr) υ: 3251 (NH) cm^{-1}; ^1H NMR (DMSO-d_6) δ: 1.75 (s, 3H, CH_3), 7.12–7.37 (m, 14H, Ar-H), 8.14(1H, d, pyrimidine-H), 8.59 (1H, d, pyrimidine-H), 11.59 (br., s, 1H, NH, D_2O exchangeable); ^{13}C NMR (DMSO-*d*6): δ 12.5 (CH_3), 108.2, 114.4, 117.8, 122.0, 125.1, 125.7, 126.0, 126.5, 126.8, 126.9, 127.8, 128.1, 128.2, 128.7, 129.5, 130.7, 132.1, 135.1, 137.0, 139.8, 140.3, 145.9(Ar-C) ppm; MS *m/z* (%): 401 (M^++1, 67), 400 (M^+, 100), 355 (67), 296 (85), 229 (58), 128 (69),

64 (60). Anal. Calcd for $C_{27}H_{20}N_4$ (400.47): C, 80.98; H, 5.03; N, 13.99. Found: C, 80.77; H, 5.01; N, 13.67%.

4.1.5.5. 5-(2-Methyl-4,5-diphenyl-1H-pyrrol-3-yl)-2-thioxo-2,3-dihydropyrido[2,3-d]pyrimidin-4(1H)-one (**18**): Yield 72%, mp 326-328 °C; IR (KBr) *υ*: 3423, 3316, 3203 (3 NH), 1668 (CO)cm^{-1}; ^{1}H NMR (DMSO-d_6) δ: 1.75 (s, 3H, CH_3), 7.11–7.37 (m, 11H, Ar-H, NH), 7.59 (d, 1H, pyridine-H3), 8.38 (d, 1H, pyridine- H2), 11.59, 12.46 (br., s, 2H, 2NH, D_2O exchangeable) ppm; MS *m/z* (%): 411 (M^++1, 73), 410 (M^+, 85), 362 (86), 271 (100), 220 (97), 181 (97), 87 (81). Anal. Calcd for $C_{24}H_{18}N_4OS$ (410.49): C, 70.22; H, 4.42; N, 13.65. Found: C, 70.01; H, 4.38; N, 13.36%.

4.1.6. **Alternative synthesis of compounds 10**. A solution of sodium (2-methyl-4,5-diphenyl-1*H*-pyrrol-3-yl)-3-oxoprop-1-en-1-olate (**5**) (0.650 g, 2 mmol) and 3-amino-4-cyanopyrazole **9** (0.216 g, 2 mmol) and piperidine acetate (1 mL) in water (3 mL) was refluxed for 10 min. After completion of the reaction, the hot reaction mixture was neutralized with acetic acid (1.5 mL), then cooled and the solid products collected by filtration and recrystallized from EtOH gave product **10** in 84% yield, which were identical in all aspects (m.p., mixed m.p. and spectra) with those obtained from reaction of enaminone **3** or **4** with **9**.

4.1.7. **Preparation of compounds 20a-c**. To a solution of **3** or **4** (5 mmol) in glacial acetic acid (20 mL) was added the appropriate active methylene compound (acetylacetone **19a** or ethyl acetoacetate **19b** or ethyl benzoylacetate **19c**) (5 mmol) and ammonium acetate (0.5 g, 6 mmol). The reaction mixture was heated under reflux for 20-30 hours. The reaction was followed by TLC. The reaction mixture poured into cold water, the solid product that precipitated was filtered off and crystallized from ethanol to give the respective product **13**. The compounds **13a-c** prepared together with their physical constant are given bellow.

4.1.7.1. 1-(2-Methyl-6-(2-methyl-4,5-diphenyl-1H-pyrrol-3-yl)pyridin-3-yl)ethanone (**20a**). Yield 70%, mp 243-245 °C; IR (KBr) *υ*: 3262 (NH), 1708 (CO)cm^{-1}; ^{1}H NMR (DMSO-d_6) δ: 1.83 (s, 3H, CH_3), 2.48 (s, 3H, CH_3), 2.68 (s, 3H, CH_3), 7.19–7.47 (m, 10H, Ar-H), 7.72 (d, 1H, pyridine-H3), 8.35 (d, 1H, pyridine- H2), 11.67 (br., s, 1H, 1NH, D_2O exchangeable); ^{13}C NMR (DMSO-*d*6): δ 13.7 (CH_3), 28.7 (CH_3), 30.4 (CH_3), 109.3, 112.1, 112.3, 117.8, 119.7, 122.0, 126.0, 126.5, 126.8, 128.1, 128.2, 130.7, 132.1, 135.1, 137.0, 145.0, 146.3 (Ar-C), 194.4 (C=O) ppm; MS *m/z* (%): 367 (M^++1, 20), 366

(M^+, 32), 260 (100), 230 (56), 189 (33), 102 (37), 77 (84). Anal. Calcd for $C_{25}H_{22}N_2O$ (366.45): C, 81.94; H, 6.05; N, 7.64. Found: C, 81.68; H, 6.01; N, 7.56%.

*4.1.7.2. Ethyl 2-methyl-6-(2-methyl-4,5-diphenyl-1H-pyrrol-3-yl)nicotinate (***20b).** Yield 74%, mp 214-216 °C; IR (KBr) *υ*: 3212 (NH), 1723 (CO)cm^{-1}; ^{1}H NMR (DMSO-d_6) *δ*: 1.35 (t, 3H, CH_3), 1.82 (s, 3H, CH_3), 2.57 (s, 3H, CH_3), 4.29 (q, 2H, CH_2), 7.19–7.51 (m, 10H, Ar-H), 7.57 (d, 1H, pyridine-H3), 8.38 (d, 1H, pyridine- H2), 11.67 (br., s, 1H, 1NH, D_2O exchangeable) ppm; ^{13}C NMR (DMSO-*d*6): *δ* 10.5(CH_3),13.7(CH_3), 30.4 (CH_3), 66.0 (CH_2), 114.9, 116.5, 118.6, 122.0, 126.0, 126.5, 126.8, 128.1, 128.2, 129.1, 1296, 130.1, 130.6, 132.1, 135.1, 137.0, 140.1 (Ar-C), 173.4 (C=O) ppm; MS *m/z* (%): 397 (M^++1, 47), 396 (M^+, 96), 248 (81), 157 (74), 136 (83), 77 (100). Anal. Calcd for $C_{26}H_{24}N_2O_2$ (396.48): C, 78.76; H, 6.10; N, 7.07. Found: C, 78.65; H, 6.03; N, 7.02%.

4.1.7.3. Ethyl 6-(2-methyl-4,5-diphenyl-1H-pyrrol-3-yl)-2-phenylnicotinate (**20c**). Yield 71%, mp 266 °C; IR (KBr) *υ*: 3248 (NH), 1717 (CO)cm^{-1}; ^{1}H NMR (DMSO-d_6) *δ*: 1.24(t, 3H, CH_3), 1.76 (s, 3H, CH_3), 4.29 (q, 2H, CH_2), 7.11–7.39 (m, 15H, Ar-H), 7.86 (d, 1H, pyridine-H3), 8.49 (d, 1H, pyridine-H2), 11.56 (br., s, 1H, 1NH, D_2O exchangeable) ppm; MS *m/z* (%): 459 (M^++1, 34), 458 (M^+, 100), 324(81), 203 (67), 157 (56), 77 (78). Anal. Calcd for $C_{31}H_{26}N_2O_2$ (458.55): C, 81.20; H, 5.72; N, 6.11. Found: C, 81.03; H, 5.58; N, 6.03%.

4.1.8. **Preparation of compounds 23a,b.** To compound **3** or **4** (5 mmol) in solution of sodium ethoxide in ethanol (0.12 g of sodium metal in 20 mL absolute ethanol) was added malononitrile **22a** or ethyl cyanoacetate **22b** (5 mmol). The reaction mixture was refluxed for 5 h., and then poured into ice-cold water. The solution was acidified with HCl (1 M) and the solid that deposited was filtered and crystallized from ethanol to give the respective compounds **23a, b**.

4.1.8.1. 6-(2-Methyl-4,5-diphenyl-1H-pyrrol-3-yl)-2-oxo-1,2-dihydropyridine-3-carbonitrile (**23a**). Yield 75%, mp 203-205 °C; IR (KBr) *υ*: 3406, 3212 (2NH), 2214 (CN), 1657 (CO)cm^{-1}; ^{1}H NMR (DMSO-d_6) *δ*: 1.82 (s, 3H, CH_3), 7.19–7.61 (m, 10H, Ar-H), 8.01 (d, 1H, pyridine-H), 8.57 (d, 1H, pyridine-H), 11.66 (br., s, 1H, 1NH, D_2O exchangeable), 12.29 (br., s, 1H, 1NH, D_2O exchangeable) ppm; MS *m/z* (%): 352 (M^++1, 57), 351 (M^+, 76), 270 (100), 210 (79), 144 (80), 101 (61), 63 (71). Anal. Calcd for $C_{23}H_{17}N_3O$ (351.40): C, 78.61; H, 4.88; N, 11.96. Found: C, 78.43; H, 4.39; N, 11.72%.

4.1.8.2. Ethyl 6-(2-methyl-4,5-diphenyl-1H-pyrrol-3-yl)-2-oxo-1,2-dihydropyridine-3-carboxylate (**23b**). Yield 77%, mp 189-191 °C; IR (KBr) *υ*: 3387, 3231 (2NH),1712, 1657 (2CO)cm^{-1}; ^{1}H NMR (DMSO-d_6) *δ*: 1.34 (t, 3H, CH_3), 1.82 (s, 3H, CH_3), 4.24 (q, 2H, CH_2), 7.11–7.56 (m, 10H, Ar-H), 8.05 (d, 1H, pyridine-H), 8.56 (d, 1H, pyridine-H), 11.56 (br., s, 1H, 1NH, D_2O exchangeable), 12.13 (br., s, 1H, 1NH, D_2O exchangeable) ppm; MS *m/z* (%): 352 (M^++1, 57), 351 (M^+, 76), 270 (100), 210 (79), 144 (80), 101 (61), 63 (71). Anal. Calcd for $C_{25}H_{22}N_2O_3$ (398.45): C, 75.36; H, 5.57; N, 7.03. Found: C, 75.23; H, 5.53; N, 6.91%.

4.1.9. **Alternative synthesis of compound 23a.** To a solution of **3** (2.11 g, 5 mmole) in ethanolic sodium ethoxide solution (0.12 g. 5 mmol of sodium metal in 20 ml absolute ethanol) was added cyanoacetamide **24a** (0.42 g, 5 mmol). The reaction mixture was refluxed for 20 h., and the solid that precipitated was filtered off and washed with water then crystallized from ethanol to give compound **23a** which was found identical in all respects with that compound produced from reaction of compound **3** with malononitrile.

4.2. **Pharmacology**

4.2.1. Biological assay In vitro ubiquitination assay. The expression of recombinant glutathione-*S*-transferase-tagged MDM2 (GST-MDM2) was induced in 25 mL culture of exponentially growing Escherichia coli BL21 cells (OD600 0.6) by 1 mM isopropyl-thio-β-D-galactoside for 3 h. Glutathione-S-transferase-MDM2 was purified on glutathione-sepharose beads (Amersham). The beads were washed with 50 mM Tris (pH 7.5).

Fluorescent ubiquitin (5 µg; Invitrogen), 50 ng mammalian E1 (Enzo), 200 ng human recombinant UbcH5B E2 (Enzo) and 200 ng His-p53 (Enzo) were mixed with reaction buffer [50 mM Tris pH 8, 2 mM dithiothreitol, 5 mM $MgCl_2$, 2 mM adenosine triphosphate (ATP)]. A dose titration of each MPD compound or dimethyl sulfoxide (DMSO) was added to the mixture and the mixture was pipetted onto GS4b-MDM2 beads. The reaction was incubated at 37 °C, shaking at 1200 r.p.m. for 1 h and then stopped by the addition of 3X sodium dodecyl sulfate sample buffer. Free fluorescent ubiquitin was washed off and total fluorescent ubiquitin signal was measured on a monochromator plate reader (Safire).

4.2.2. For non-fluorescent in vitro ubiquitination assays: the procedure was as above except 5 µg unlabeled ubiquitin (Enzo) was used. Ten micrometers of each tested compound or DMSO was added to the mixture and then pipetted onto GS4b-MDM2 beads. After incubation, as described previously, reaction products were resolved by sodium dodecyl sulfate–polyacrylamide gel electrophoresis and analyzed by western blotting with anti-p53 DO-1. For the MDM2 RING autoubiquitination assay, GS4b-MDM2 RING beads were prepared as above and used in place of the full-length MDM2.

Abbreviations: ARF, alternative reading frame; DMEM, Dulbecco's modified Eagle's medium; DMSO, dimethyl sulfoxide, HLI98, HDM2 ligase inhibitor 98 class.

For the MDM2 autoubiquitination assay, the procedure was performed as detailed above except that no His-p53 was added to the reaction and western blotting was with Ab1 and Ab2 antibodies.

For the Cbl autoubiquitination assay, bacterially expressed full-length Cbl was used in a reaction with the previously described quantities of E1, E2 and ubiquitin. Ubiquitinated Cbl was detected by western blotting using antiubiquitin antibody (Sigma clone 6C1).

4.3. **Molecular Modeling**. The structures of newly synthesized compounds were built with Sybyl-X software and minimized to 0.01kcal/mol by the Powell method, using Gasteiger-Hückel charges and the Tripos force field. The proteins coordinates have been downloaded from Protein Data Bank website (PDB IDs: 1t4f). The water molecules and all other substructures including p53 residues were removed. The hydrogen atoms were added and the energy of the protein was minimized using the Amber force field with Amber charges. The energy-optimized lignads were docked into the binding site (close to atomno. 654) in the protein using GOLD [36]. The parameters were set as the default values for GOLD. The maximum distance between hydrogen bond donors and acceptors for hydrogen bonding was set to 3.5 Å. After docking, the top three poses conformations of each lignad were merged into the ligand-free protein. The new ligand–protein complexes were subsequently subjected to energy minimization using the Amber force field with Amber charges. The energy minimization, in all cases, was performed using the Powell method with a 0.05 kcal/(mol Å) energy gradient convergence criterion and a distance dependent dielectric function.

The authors have declared no conflict of interest.

References

[1] K. H. Vousden, D. P. Lane, p53 in health and disease. Nat. Rev. Mol. Cell. Biol., 8 (2007) 275-283.

[2] D. R. Zweitzig, N. Shcherbik, D.S. Haines, Retraction for D. R. Zweitzig, N. Shcherbik, and D. S. Haines: AAA ATPase P97 and adaptor UBXD1 suppress MDM2 ubiquitination and degradation and promote constitutive P53 turnover. Mol. Biol. Cell, 19(11) (2008) 5029.

[3] X.Wang, X. Jiang, Mdm2 and MdmX partner to regulate p53. FEBS lett., 586(10) (2012) 1390-1396.

[4] S.G. Dastidar, D. Raghunathan, J. Nicholson, T.R. Hupp, D.P. Lane, C.S. Verma, Chemical states of the N-terminal "lid" of MDM2 regulate p53 binding: simulations reveal complexities of modulation. Cell cycle, 10(1) (2011) 82-89.

[5] S. Fang, J. P. Jensen, R. L. Ludwig, K. H. Vousden, A. M. Weissman, Mdm2 is a RING finger-dependent ubiquitin protein ligase for itself and p53. J. Biol. Chem., 275 (2000) 8945-8951.

[6] Q. Yu, Y. Li, K. Mu, Z. Li, Q. Meng, X. Wu, et al., Amplification of Mdmx and overexpression of MDM2 contribute to mammary carcinogenesis by substituting for p53 mutations. Diagn. Pathol., 9 (2014) 71.

[7] D. Baunoch, L. Watkins, A. Tewari, M. Reece, L. Adams, R. Stack, et al., MDM2 overexpression in benign and malignant lesions of the human breast. Int. J. Oncol., 8(5) (1996) 895-899.

[8] J. S. Wunder, K. Eppert, S. R. Burrow, N. Gokgoz, R.S. Bell, I. L. Andrulis, Co-amplification and overexpression of CDK4, SAS and MDM2 occurs frequently in human parosteal osteosarcomas. Oncogenes, 18(3) (1999) 783-788.

[9] M. Zhou, A. M.Yeager, S. D. Smith, H. W. Findley, Overexpression of the MDM2 gene by childhood acute lymphoblastic leukemia cells expressing the wild-type p53 gene. Blood, 85(6) (1995) 1608-1614.

[10] P. Zhao, D. Wang, Y. Gao, Z. Yang, X. Li, Overexpression of MDM2, p53, and NCAM proteins in human radiation-induced skin ulcers. J. Environ. Pathol., Toxicol. Oncol., 17(2) (1998) 125-127.

[11] W. Biernat, P. Kleihues, Y. Yonekawa, H. Ohgaki, Amplification and overexpression of MDM2 in primary (de novo) glioblastomas. J. Neuropathol. Exp. Neurol., 56(2) (1997) 180-185.

[12] Y.T. Cheng, Y. L. Li, J.D. Wu, S. B. Long, T.S.Tzai, C.C. Tzeng, et al. Overexpression of MDM2 mRNA and mutation of the p53 tumor suppressor gene in bladder carcinoma cell lines. Mol. Carcinog., 13(3) (1995) 173-181.

[13] A. Das, W. L. Tan, J. Teo, D. R. Smith, Overexpression of MDM2 and p53 and association with progesterone receptor expression in benign meningiomas. Neuropathology, 22(3) (2002) 194-199.

[14] A. Esteve, T. Lehman, W. Jiang, I. B.Weinstein, C.C. Harris, A. Ruol, et al. Correlation of p53 mutations with epidermal growth factor receptor overexpression and absence of MDM2 amplification in human esophageal carcinomas. Mol. Carcinog., 8(4) (1993) 306-311.

[15] M. H. Kubbutat, S. N. Jones, K. H. Vousden, Regulation of p53 stability by MDM2. Nature, 387 (1997) 299-303.

[16] M. P. Dickens, R. Fitzgerald, P. M. Fischer, Small-molecule inhibitors of MDM2 as new anticancer therapeutics. Semin. Cancer Biol., 20 (2010) 10-18.

[17] S.H.Tu, C.H.Wu, L. C. Chen, C.S. Huang, H. W. Chang, C.H. Chang, et al. In vivo antitumor effects of 4,7-dimethoxy-5-methyl-1,3-benzodioxole isolated from the fruiting body of Antrodia camphorata through activation of the p53-mediated p27/Kip1 signaling pathway. J. Agric. Food Chem., 60(14) (2012) 3612-3618.

[18] Y. Yang, R. L. Ludwig, J. P. Jensen, S. A. Pierre, M. V. Medaglia, I. V. Davydov, Y.J. Safiran, P. Oberoi, J. H. Kenten, A. C. Phillips, A. M. Weissman, K. H. Vousden, Small molecule inhibitors of HDM2 ubiquitin ligase activity stabilize and activate p53 in cells. Cancer Cell, 7 (2005) 547-559.

[19] J. Kitagaki, K. K. Agama, Y. Pommier, Y. Yang, A. M. Weissman, Targeting tumor cells expressing p53 with a water-soluble inhibitor of HDM2. Mol. Cancer Ther. 7 (2008) 2445-2454.

[20] J. M. Wilson, G. Henderson, F. Black, A. Sutherland, R. L. Ludwig, K. H. Vousden, D. Robins, Synthesis, characterisation and anti-protozoal activity of carbamate-derived polyazamacrocycles. J. Bioorg. Med. Chem., 15 (2007) 77-86.

[21] Y. Ji, S. Majumder, M. Millard, R. Borra, T. Bi, A.Y. Elnagar, et al. In vivo activation of the p53 tumor suppressor pathway by an engineered cyclotide. J. Am. Chem. Soc., 135(31) (2013) 11623-11633.

[22] R. C. Poulsen, A.C. Watts, R. J. Murphy, S. J. Snelling, A. J. Carr, P. A. Hulley, Glucocorticoids induce senescence in primary human tenocytes by inhibition of sirtuin 1 and activation of the p53/p21 pathway: in vivo and in vitro evidence. Ann. Rheum. Dis. (2013) Jun. doi: 10.1136/annrheumdis-2012-203146

[23] L.T. Vassilev, B.T.Vu, B. Graves, D. Carvajal, F. Podlaski, Z. Filipovic, et al. In vivo activation of the p53 pathway by small-molecule antagonists of MDM2. Science, 303 (2004) 844-848.

[24] Y. Yang, R. L. Ludwig, J. P. Jensen, S. A. Pierre, M. V. Medaglia, I. V. Davydov, Y.J. Safiran, P. Oberoi, J. H. Kenten, A. C. Phillips, A. M. Weissman, K. H. Vousden, Cancer Cell, 7 (2005) 547-559.

[25] J. Kitagaki, K. K. Agama, Y. Pommier, Y. Yang, A. M. Weissman, Targeting tumor cells expressing p53 with a water-soluble inhibitor of Hdm2. Mol. Cancer Ther., 7 (2008) 2445-2454.

[26] J. M. Wilson, G. Henderson, F. Black, A. Sutherland, R. L. Ludwig, K. H. Vousden, D. *J.* Robins, Synthesis of 5-deazaflavin derivatives and their activation of p53 in cells. Bioorg. Med. Chem., 15 (2007) 77-86.

[27] S. I. Bhat, D. R. Trivedi, A catalyst- and solvent-free three-component reaction for the regioselective one-pot access to polyfunctionalized pyrroles, Tetrahedron Lett., 54 (2013) 5577-5582.

[28] T. M. A. Eldebss, S. M. Gomha, M. M. Abdulla, Regioselective Synthesis of novel substituted pyrrole with Protein kinases inhibitor activates selectively for VEGFR-2, EGFR, PKA and CHK1. Submitted for publication in J. Med. Chem., 2014.

[29] A. Cantos, P. De. March, M. M. Manas, A. Pla, F. S. Ferrando, A.Vergili, Synthesis of Pyrano[4,3-*c*]pyrazol-4(1*H*)-ones and -4(2*H*)-ones from Dehydroacetic Acid. Homo- and Heteronuclear Selective NOE Measurements for Unambiguous Structure Assignment. Bull. Chem. Soc. Jpn. 60 (1987) 4425-4431.

[30] S. M. Gomha, H. A. Abdel-Aziz, Enaminones as building blocks in heterocyclic preparations: synthesis of novel pyrazoles, pyrazolo- [3,4-*d*]pyridazines, pyrazolo[1,5-*a*]pyrimidines, pyrido[2,3- *d*]pyrimidines linked to imidazo[2,1-*b*]thiazole system. Heterocycles, 85 (2012) 2291-2303.

[31] R. E. Wasylishen, J. B. Rowbotham, T. Schaefer, Proton spin–spin coupling constants in isothiazole, isoxazole, and some of their alkyl derivatives, Can. J. Chem., 52 (1974) 833-837.

[32] Y. W. Ho, 5-(1-Pyrrolyl)-2-phenylthieno[2,3-d]pyrimidine as building block in heterocyclic synthesis: Novel synthesis of some pyrazoles, pyrimidines, imidazo[1,2-a]pyrimidines, pyrazolo[1,5-*a*]pyrimidines, pyrido-(pyrimido)pyrazolo[1,5-*a*]pyrimidines, 1,2,4-triazolo[1,5-*a*] pyrimidine and a 1,2,3,4-tetrazolo[1,5-a]pyrimidine derivative. J. Chin. Chem. Soc., 54 (2007) 1075-1085.

[33] S. M. Gomha, H. M. Abdel-aziz, An efficient synthesis of functionalized 2-(heteroaryl)-3*H*-benzo[f]chromen-3-ones and antibacterial evaluation. J. Chem. Res., 2 (2013) 298–303.

[34] W. Li-Rong, W. Shu-Wen, L. Ming, Y. Hua-Zheng, Reaction of enaminones with aminopyrazoles: Synthesis, structures and bioactivities of 7-aryl-3-cyano-2-substituted pyrazolo[1,5-*a*]pyrimidines, Chin. J. Chem., 23 (2005) 1231-1235.

[35] E. Breitmaier, Structure elucidation by NMR in Organic Chemistry, a Practical Guide, John Wiley: Chichester, UK, (1993), 27.

[36] M. L. Verdonk, J. C. Cole, M. J. Hartshorn, C. W. Murray, R. D. Taylor, Improved Protein-Ligand Docking Using GOLD. Protein: Struct. Funct. Genet., 52 (2003) 609-623.

Table 1: IC_{50} of p53 ubiquitination of the newly synthesized compounds (*in vitro)*.

Compound No	IC_{50} of p53 ubiquitination
6	0.99
7	0.97
8	0.94
10	0.91
12	0.89
14	0.84
16	0.36
18	0.44
20a	0.81
20b	0.78
20c	0.61
23a	0.57
23b	0.55
Diph. Imidazole	0.26(17)

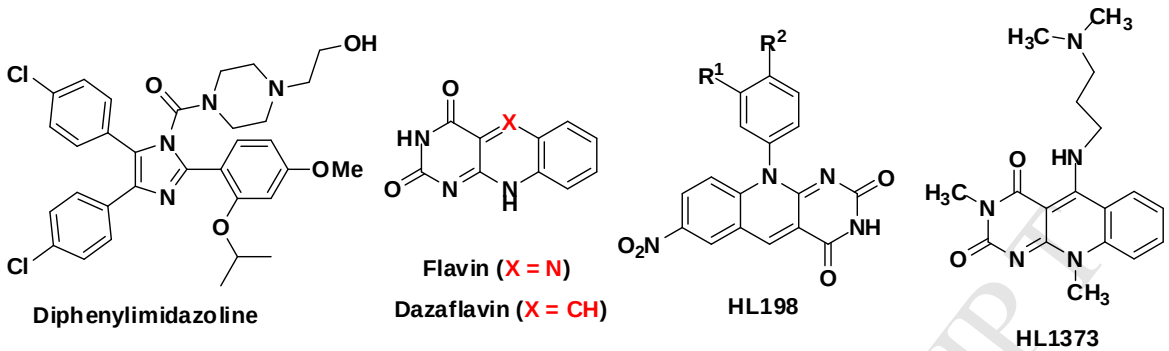

Chart 1. Chemical structures of some reported HDM2 ligase inhibitors.

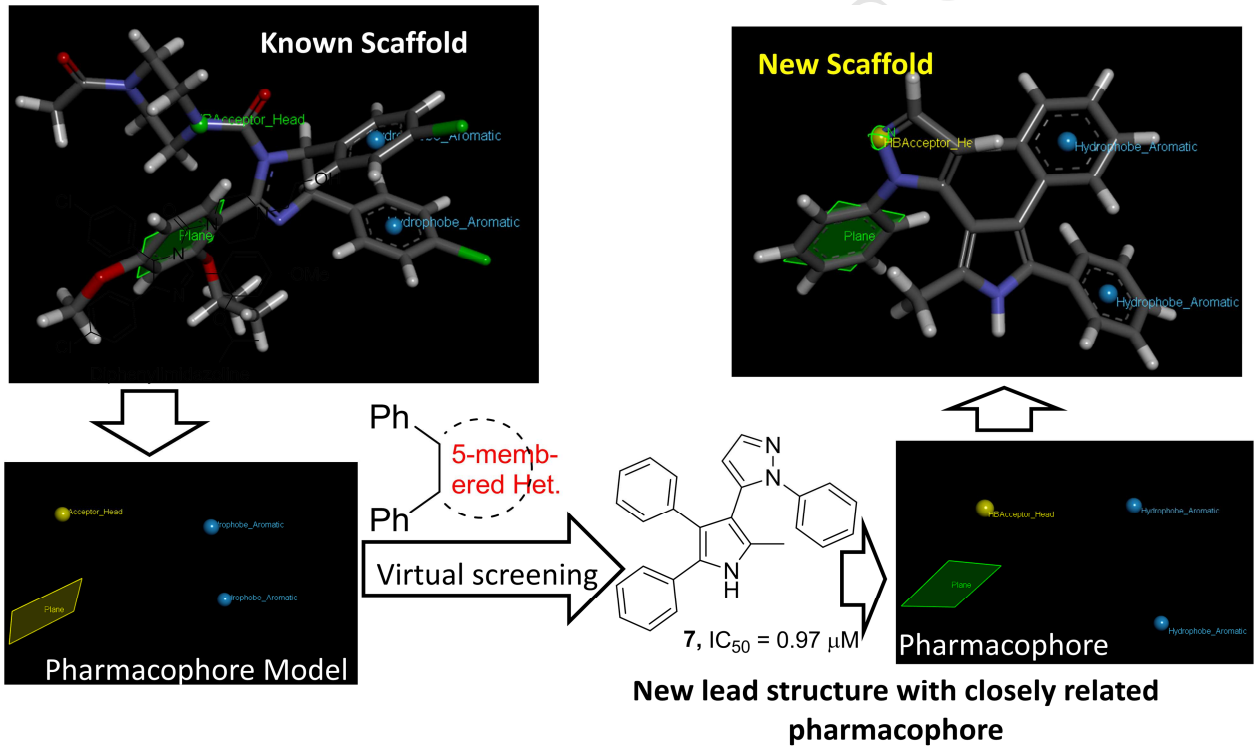

Chart 2. Work Design

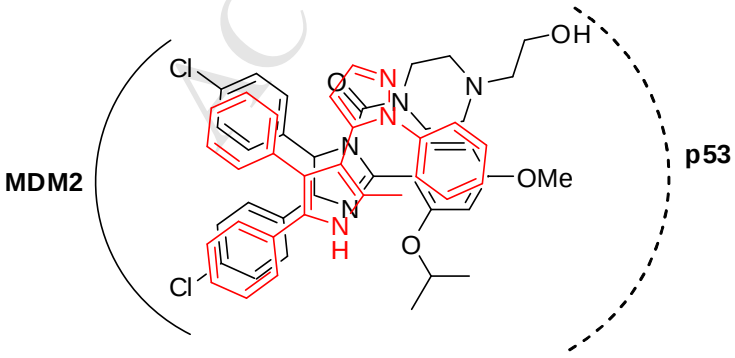

Chart 3. Alignment of reported (black) and newly (red) derived structures. The diphenyl rings of the lead structure (black) were reported to interact with MDM2 (PDB: 1rv1), leaving the other two groups facing p53.

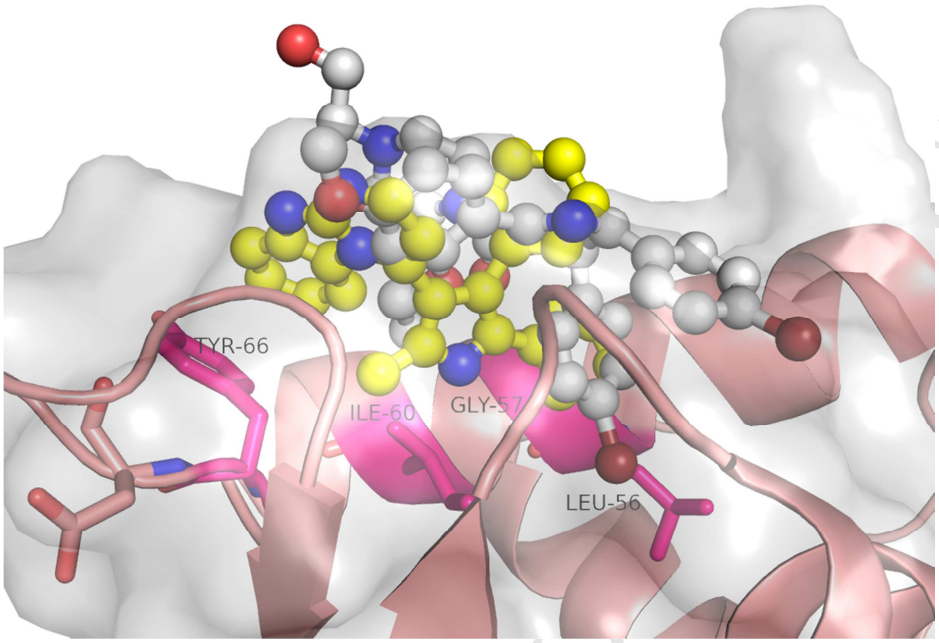

Figure 3. Hypothetical binding mode of compound **16** (colored yellow) and the reference diphenylimidazoline compound (colored light gray) in MDM2 protein (PDB: 1t4f).

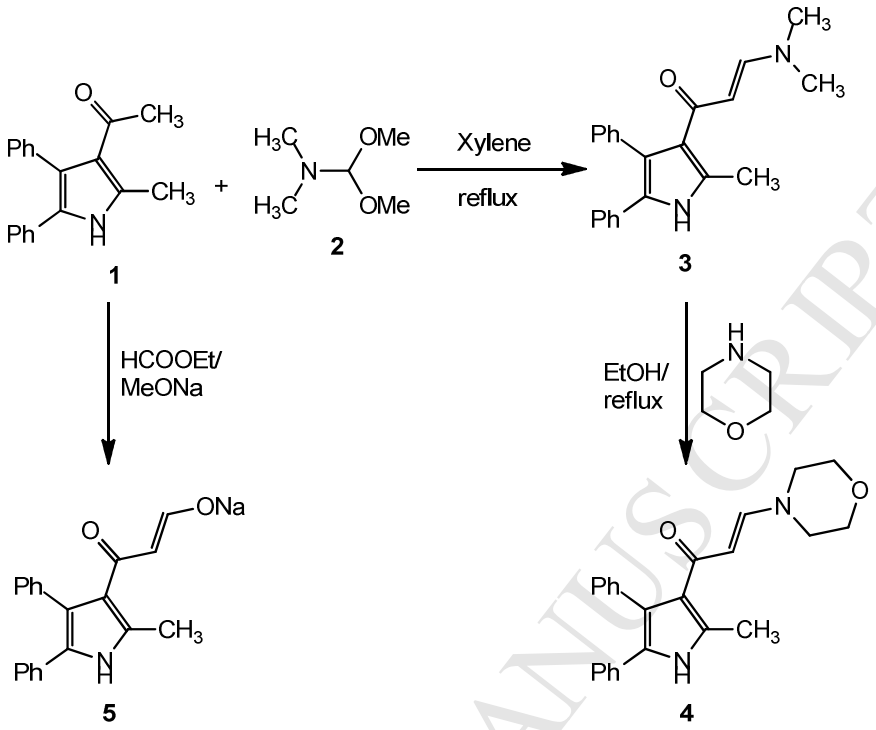

Scheme 1: Synthesis of compounds **3-5**

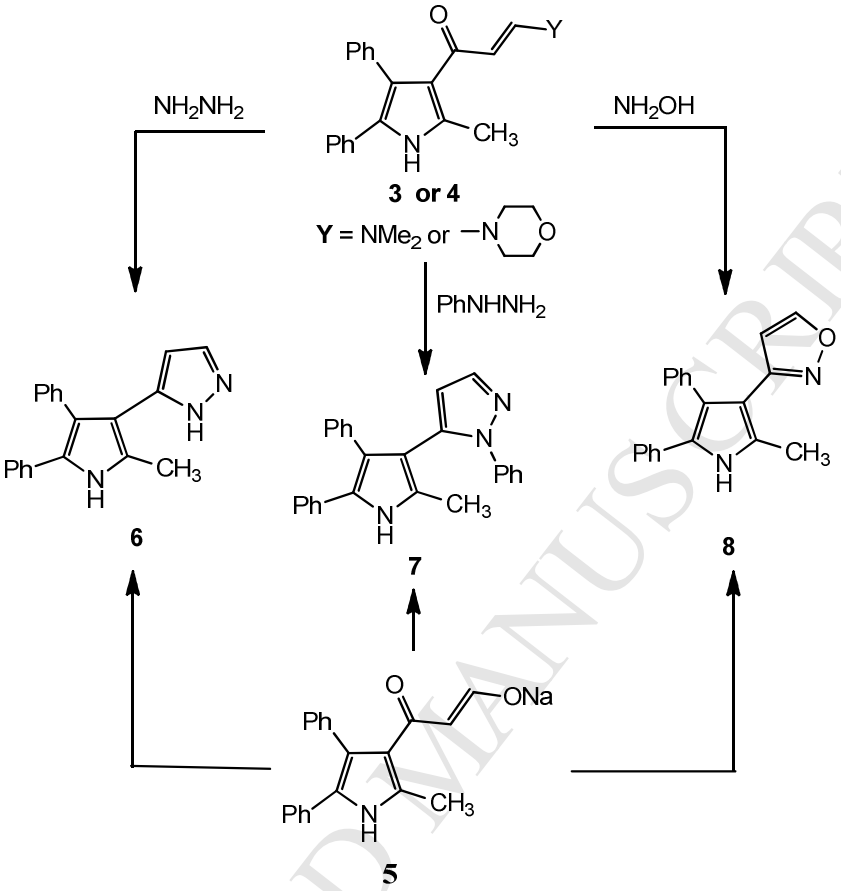

Scheme 2: Synthesis of pyrazoles **6, 7** and isoxazole **8**

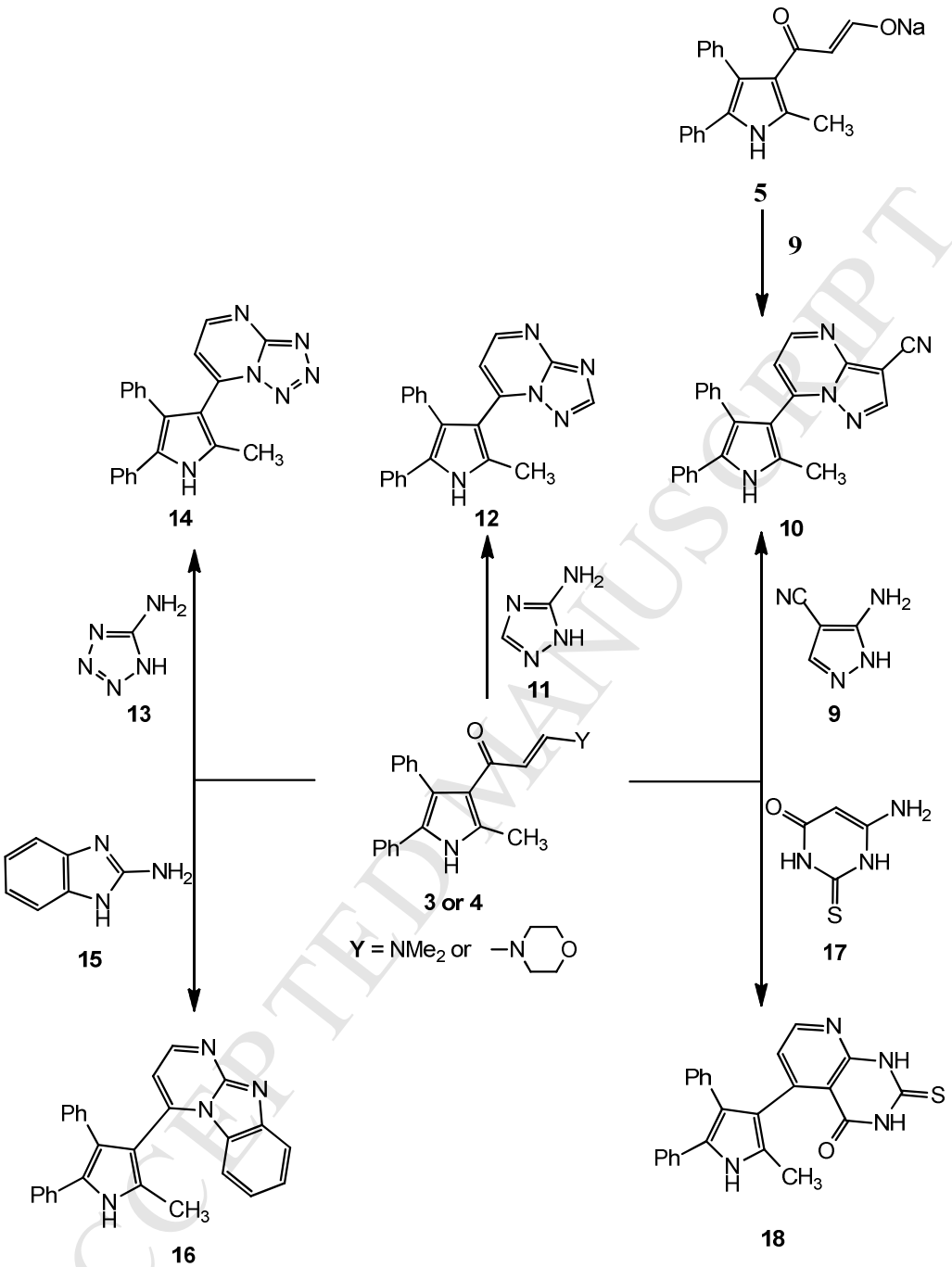

Scheme 3: Synthesis of fused pyrimidines **10, 12, 14, 16** and **18**

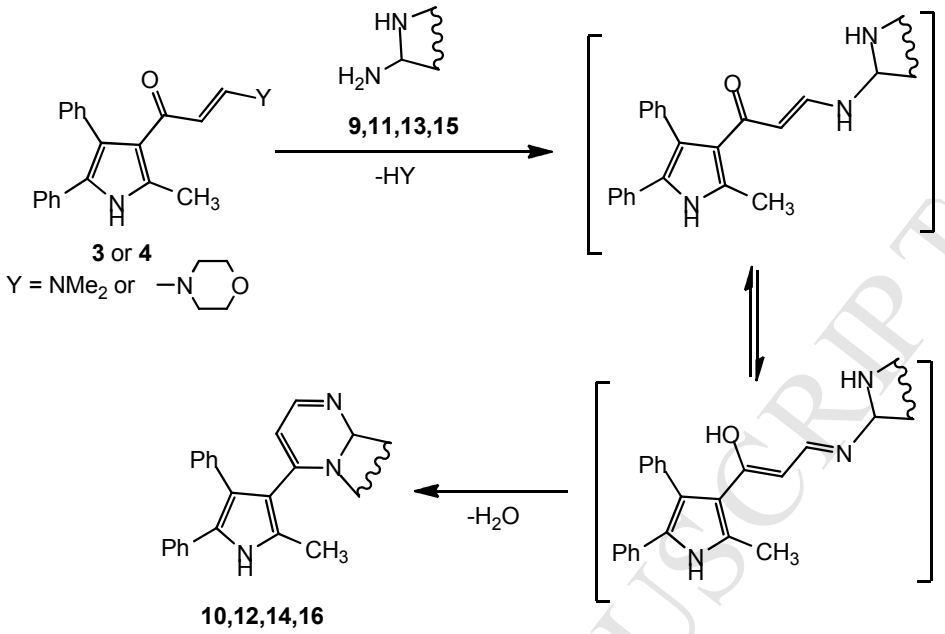

Scheme 4: Mechanism of synthesis of fused pyrimidines **10, 12, 14,** and **16**

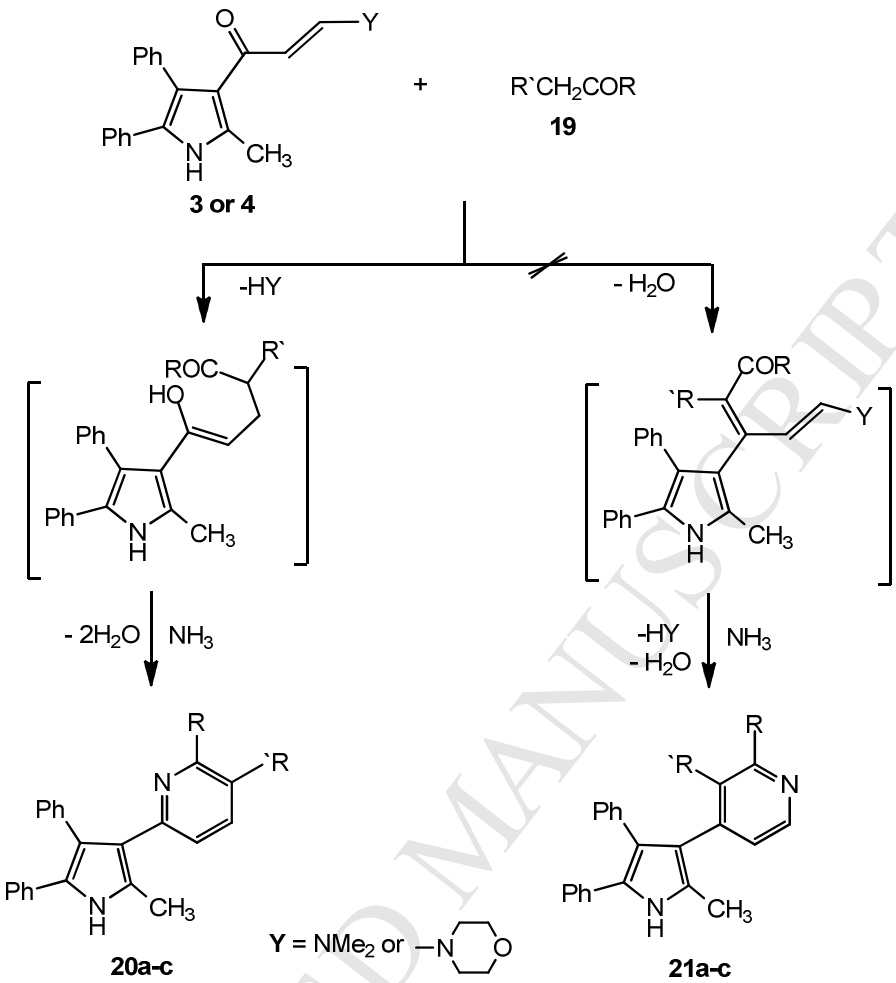

19- 21	R/ R`
a	CH_3/ $COCH_3$
b	CH_3/ COOEt
c	Ph/ COOEt

Scheme 5: Synthesis of pyridines **20a-c**

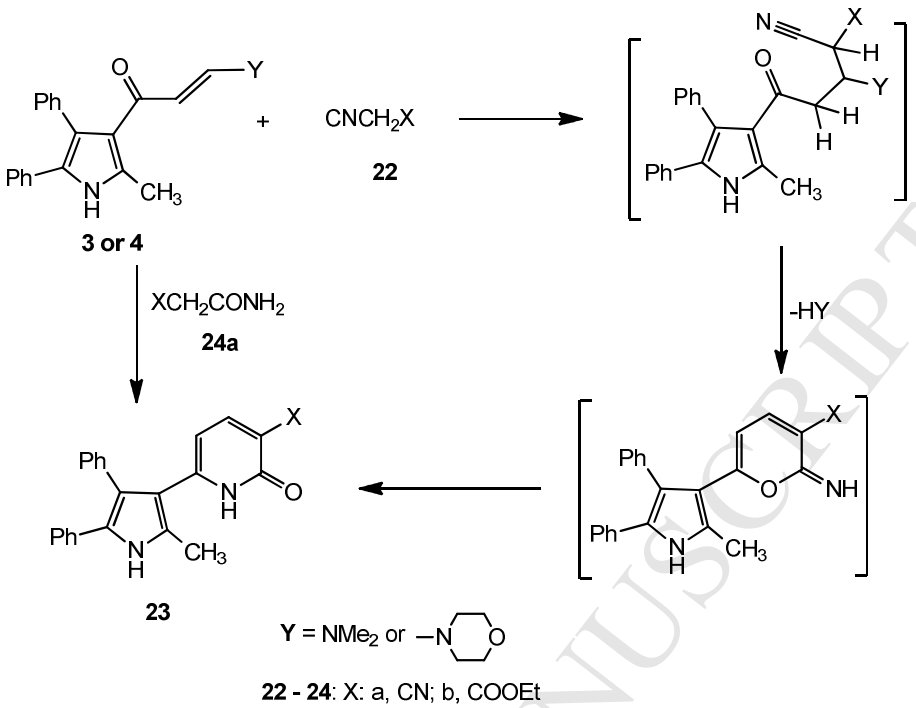

Scheme 6: Synthesis of pyridinones **23a,b**

Diphenylpyrroles: Novel p53 Activators

Sobhi M. Gomha[a*], Taha M. A. Eldebss,[a] Mohamed M. Abdulla[b] and Abdelrahman S. Mayhoub[c]

[a]*Department of Chemistry, Faculty of Science, Cairo University, Giza 12613, Egypt*

[b]*Research Unit, Saco Pharm. Co., 6th October City, Egypt*

[c]*Department of Organic Chemistry, Faculty of Pharmacy, Al-Azhar University, Cairo, 11884 Egypt*

Table of Contents

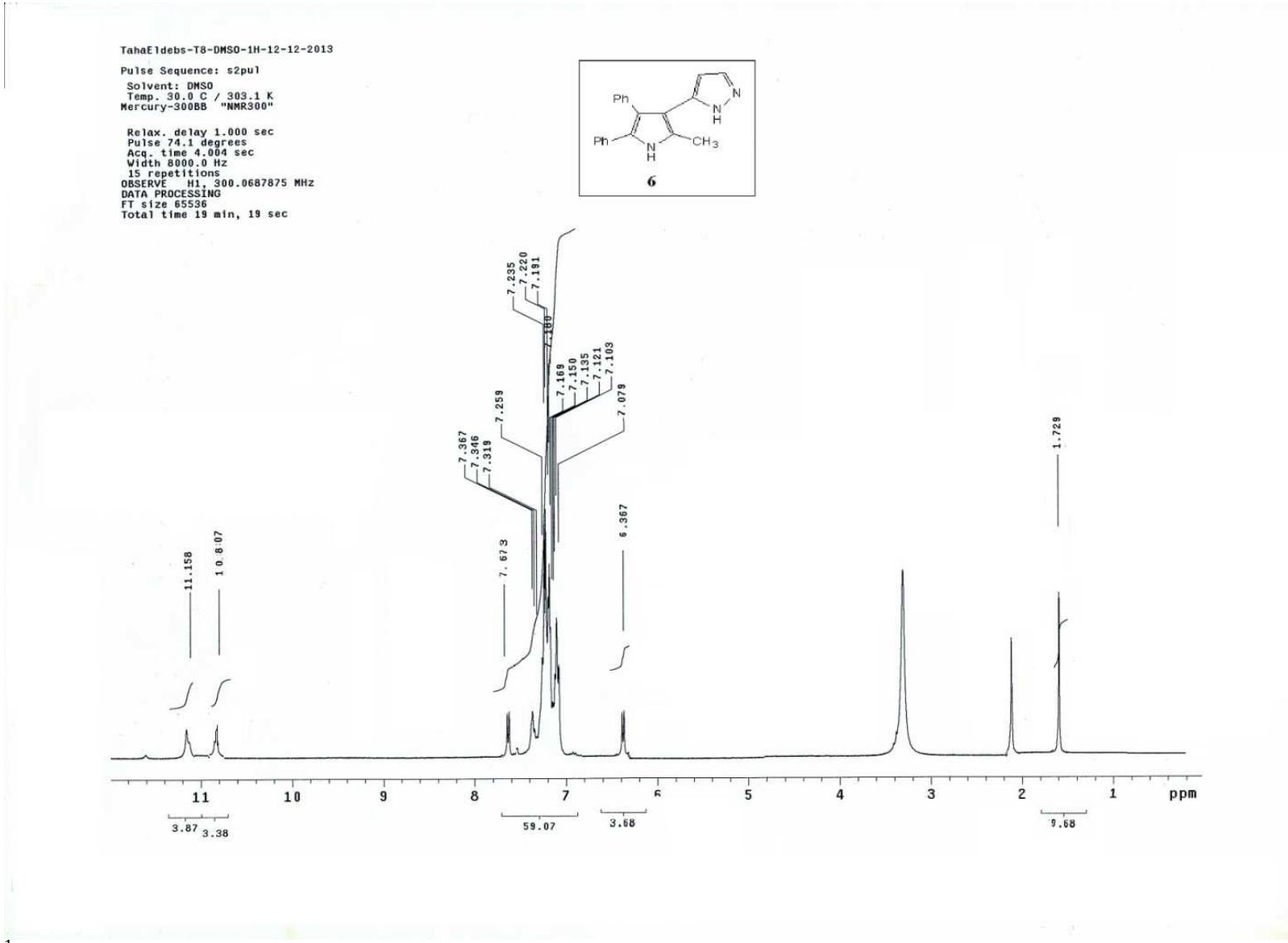

^{1}H NMR spectrum of compound **6**

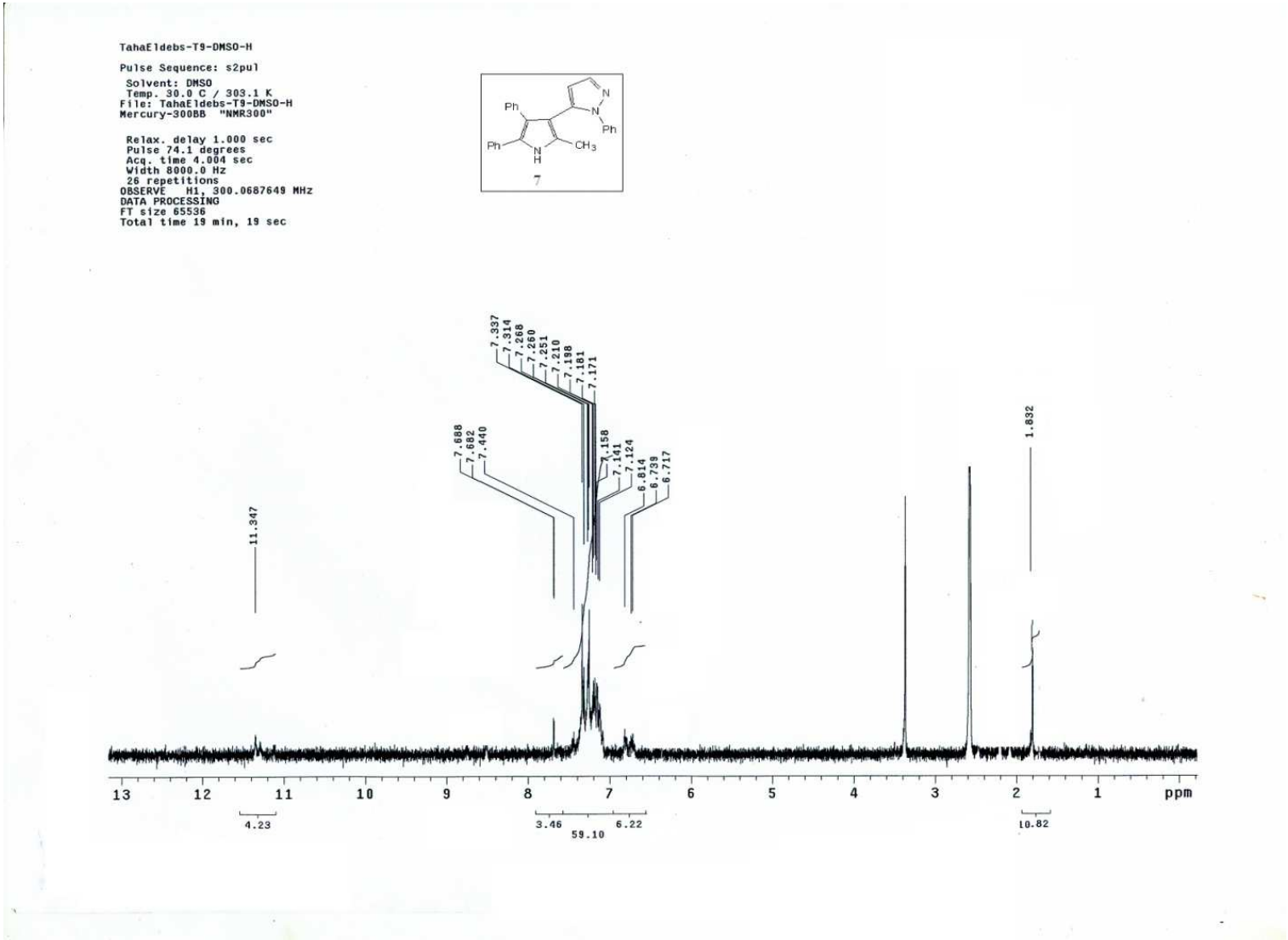

^{1}H NMR spectrum of compound **7**

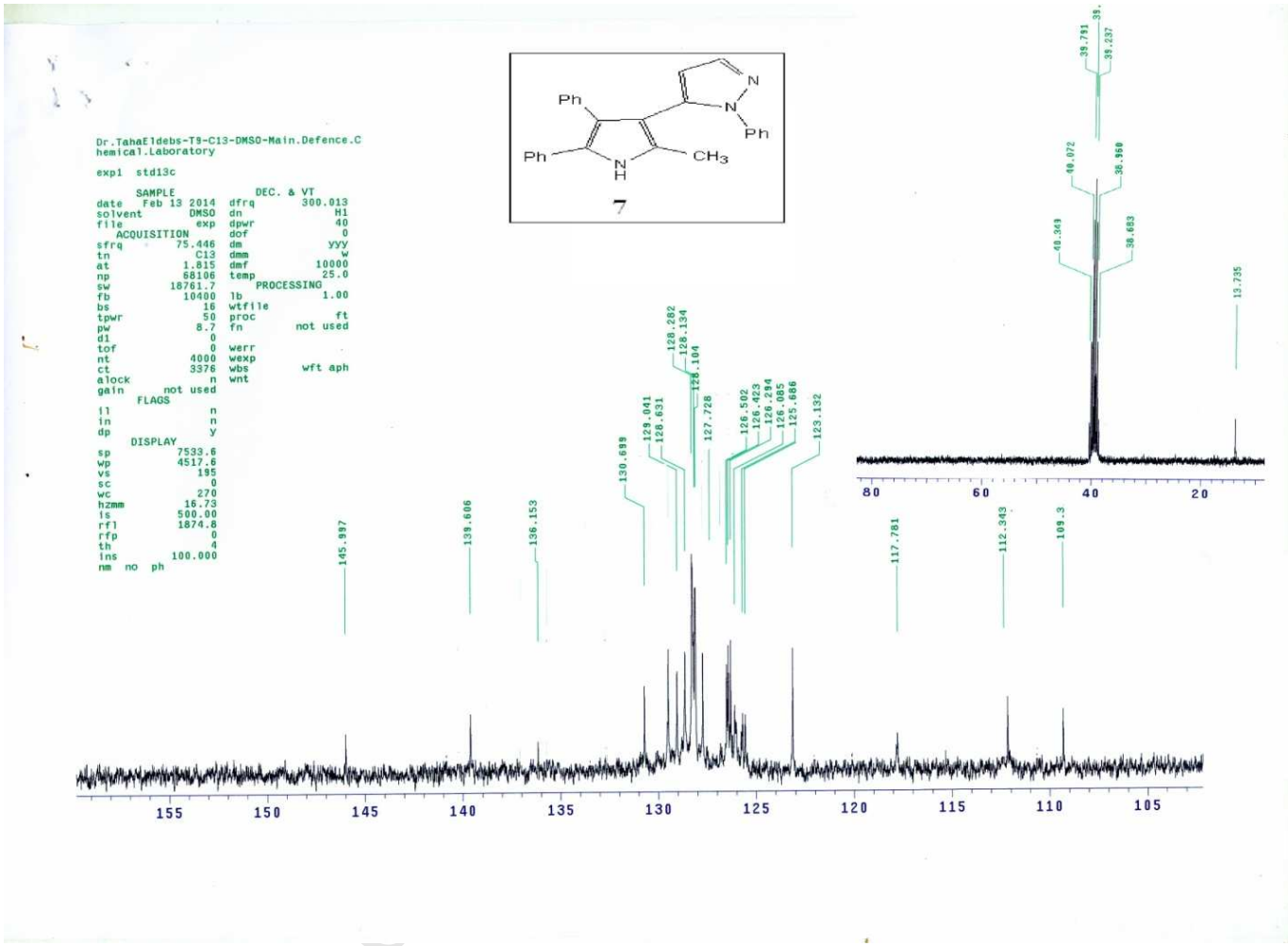

^{13}C NMR spectrum of compound **7**

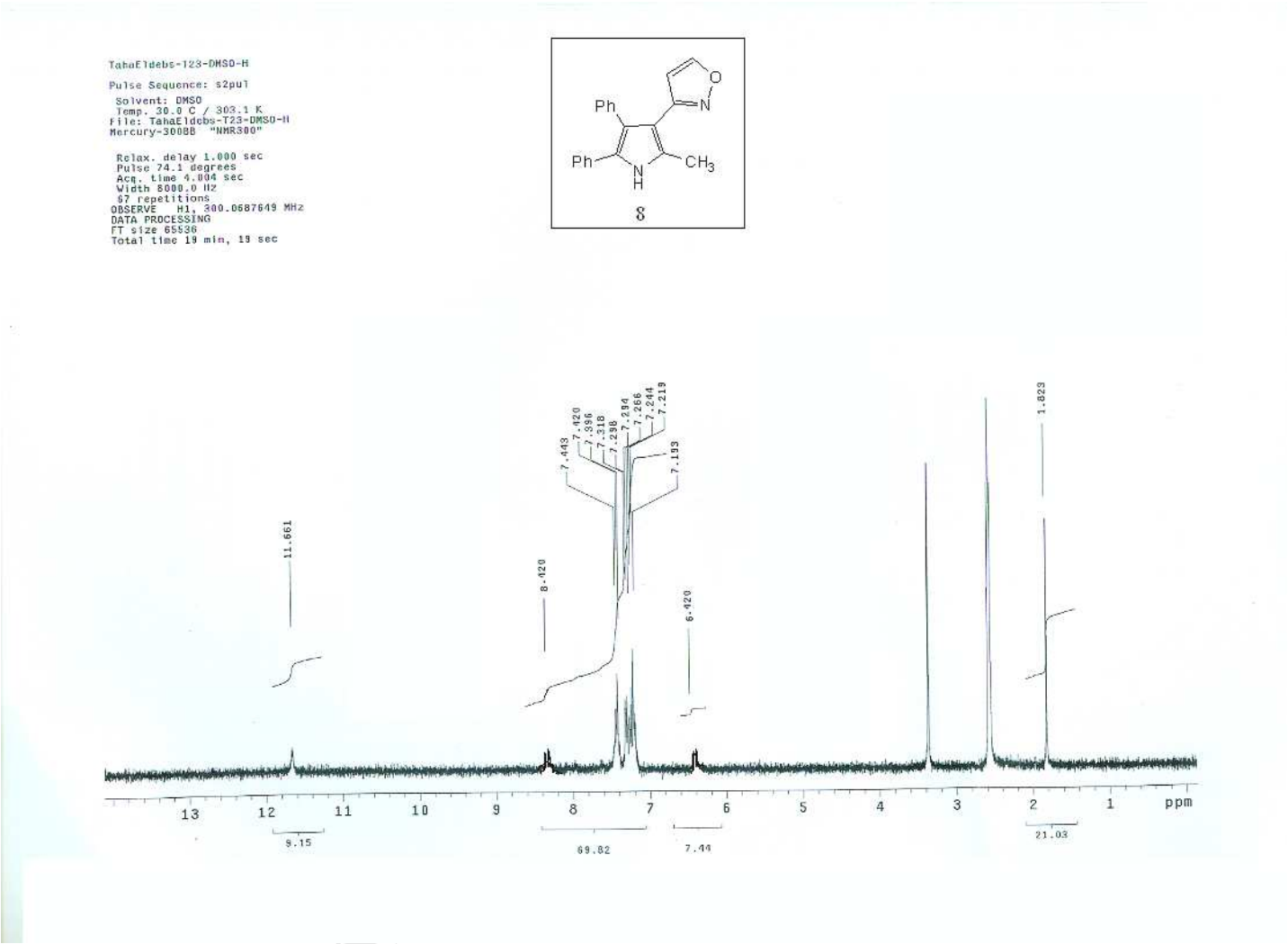

^{1}H NMR spectrum of compound **8**

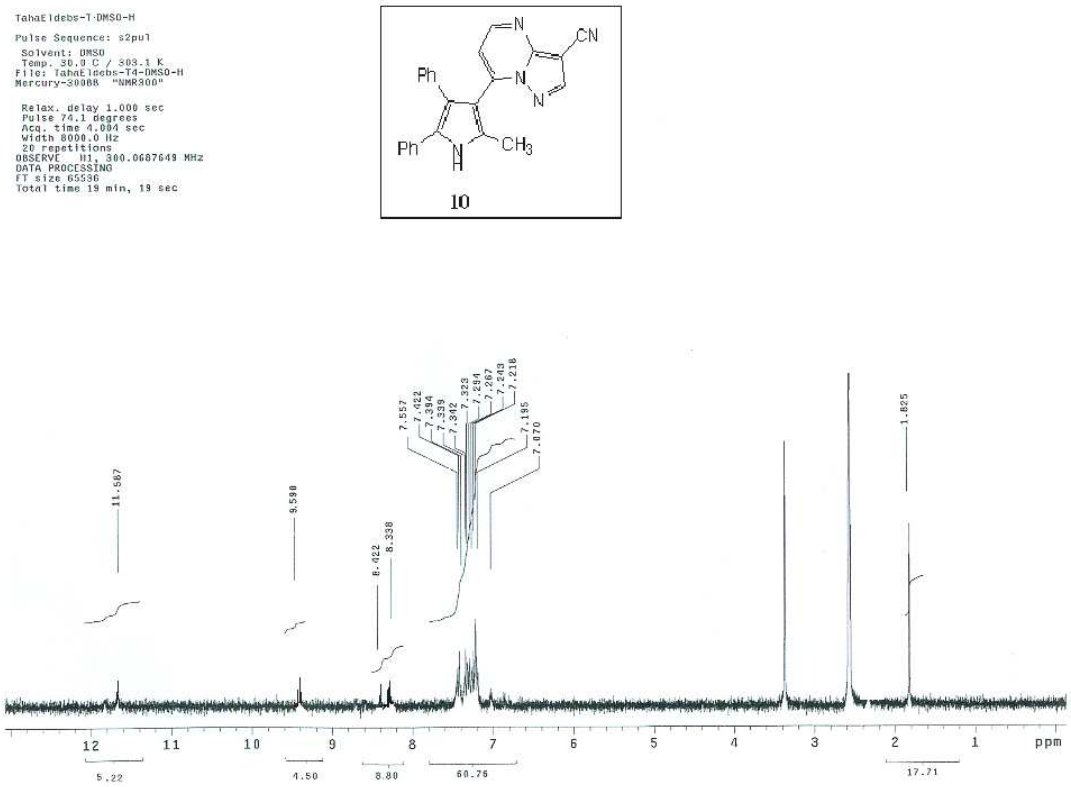

^{1}H NMR spectrum of compound **10**

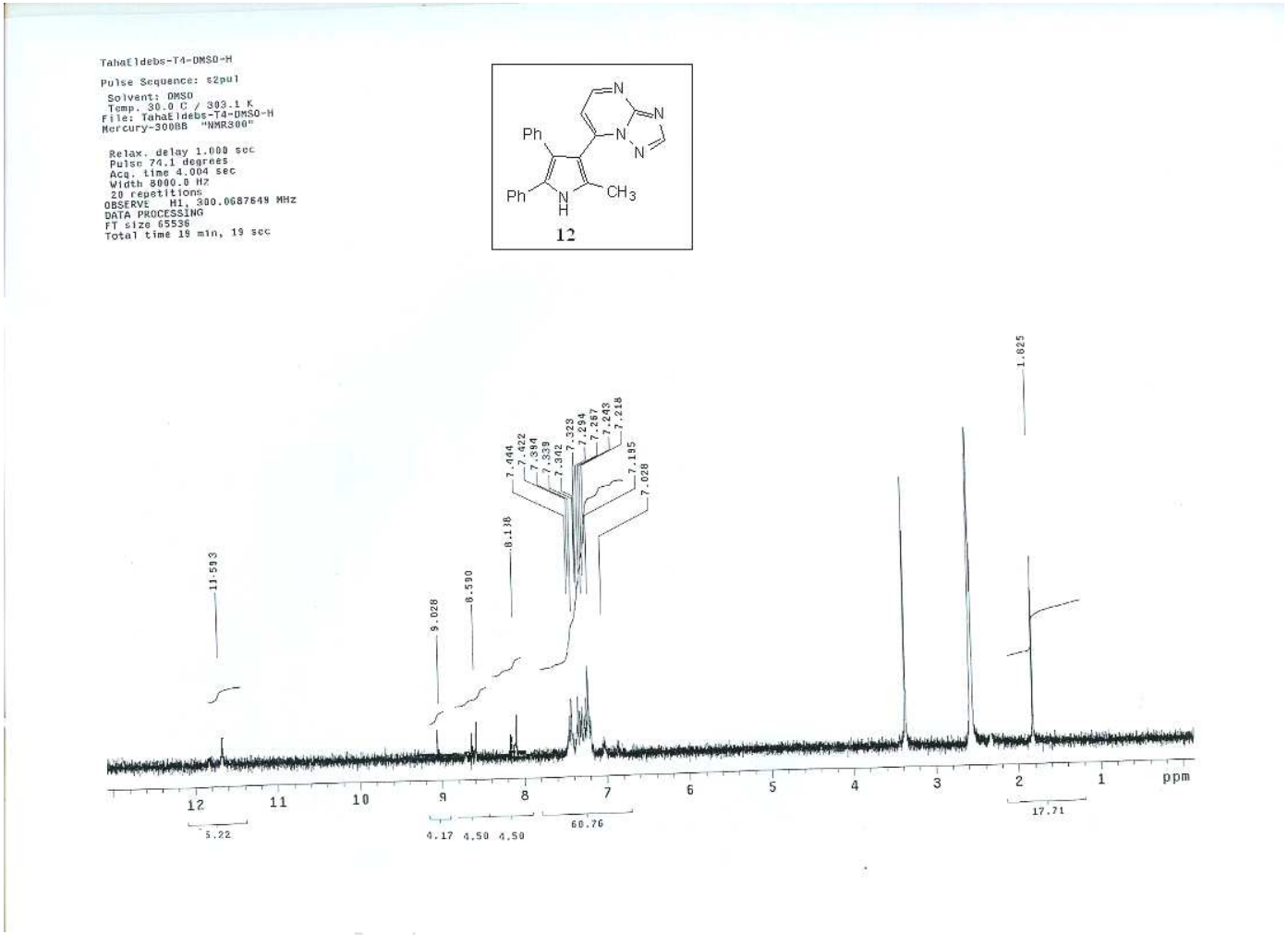

^{1}H NMR spectrum of compound **12**

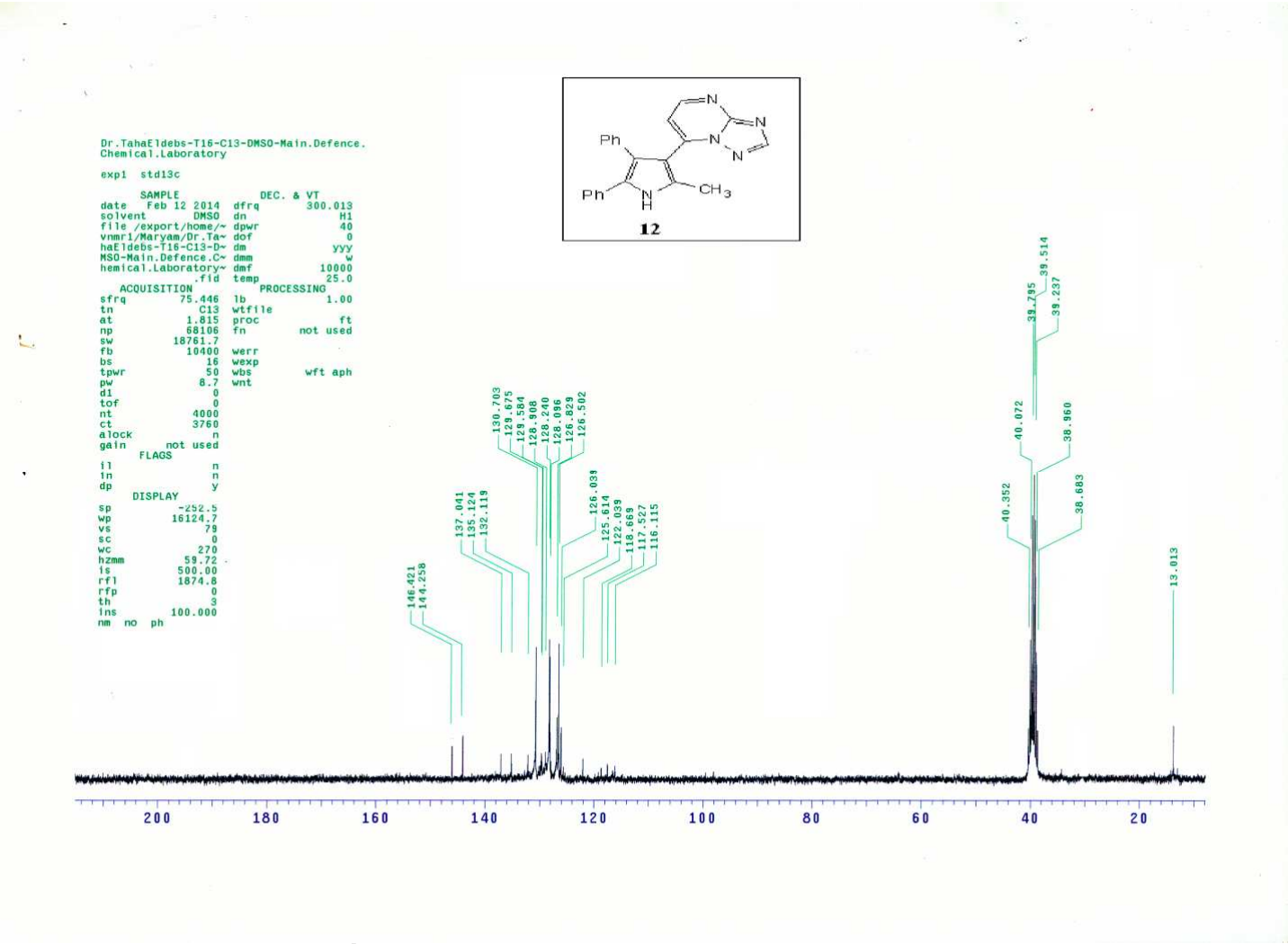

^{13}C NMR spectrum of compound **12**

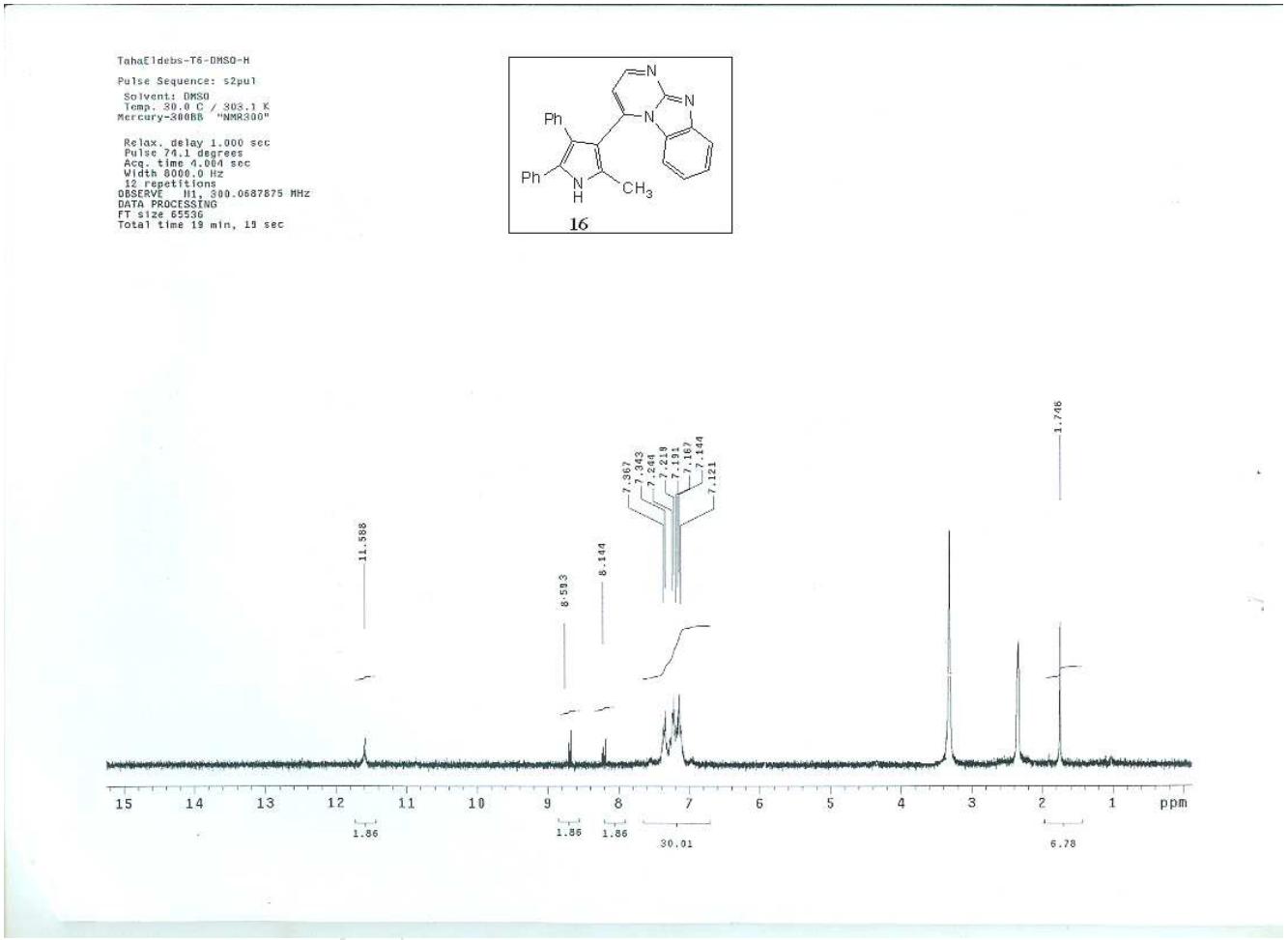

^{1}H NMR spectrum of compound **16**

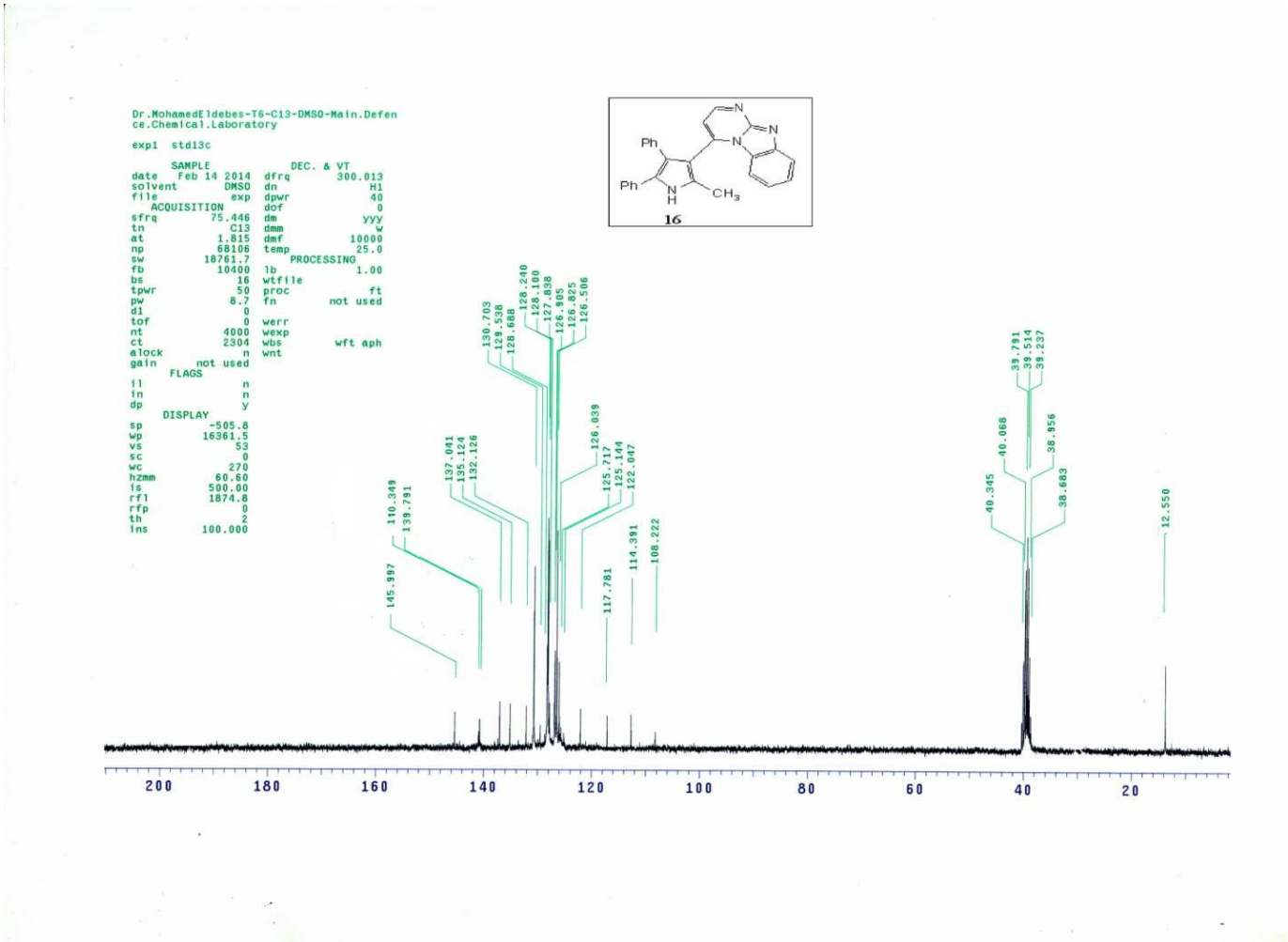

^{13}C NMR spectrum of compound **16**

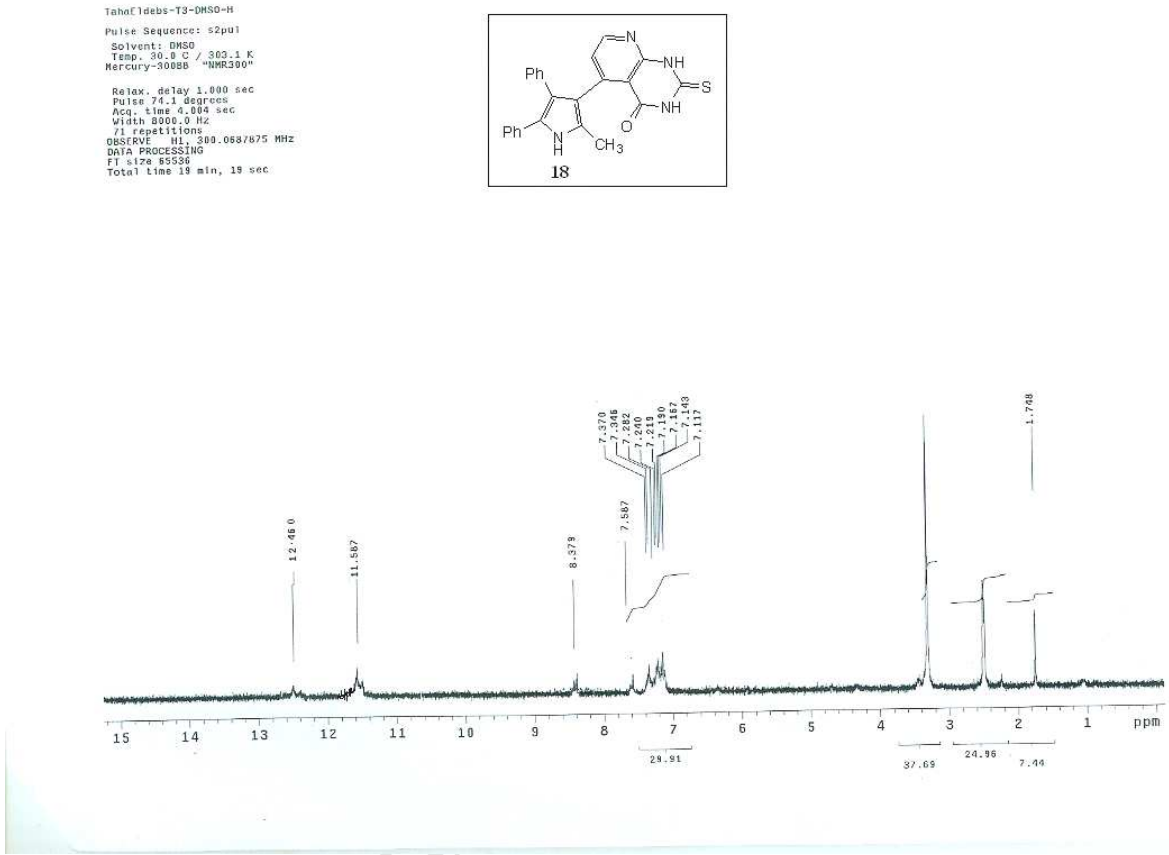

^{1}H NMR spectrum of compound **18**

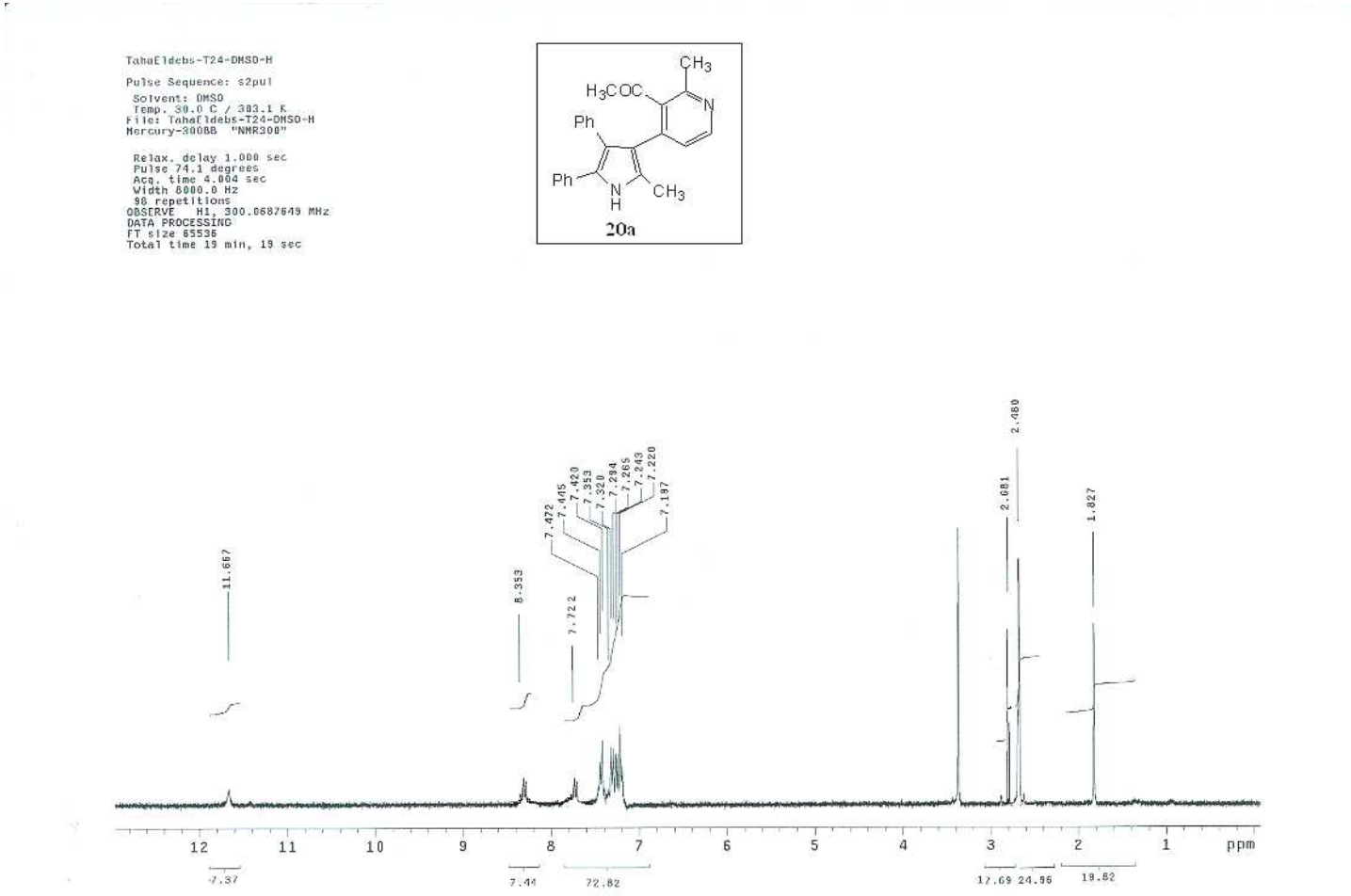

^{1}H NMR spectrum of compound **20a**

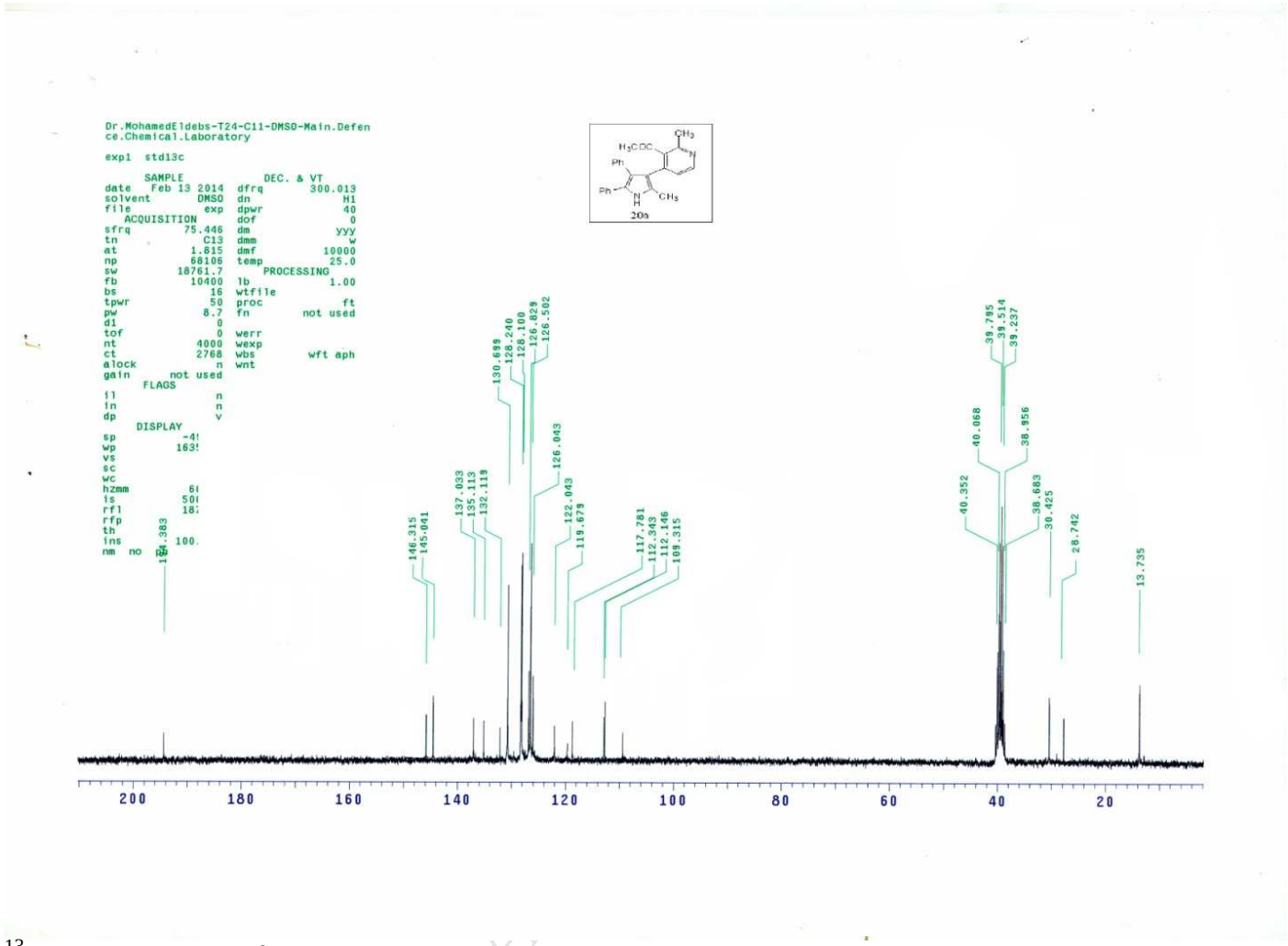

^{13}C NMR spectrum of compound **20a**

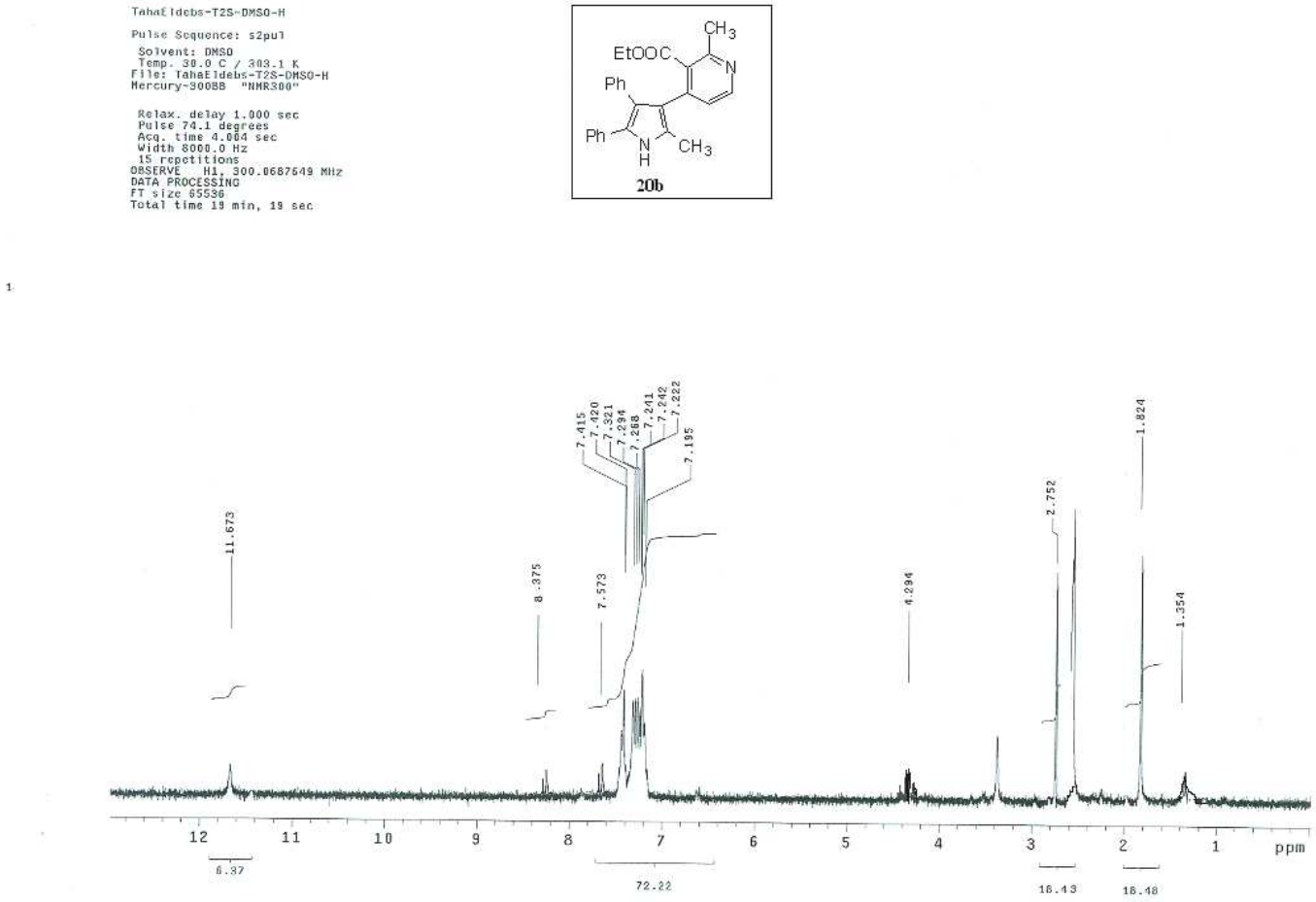

^{1}H NMR spectrum of compound **20b**

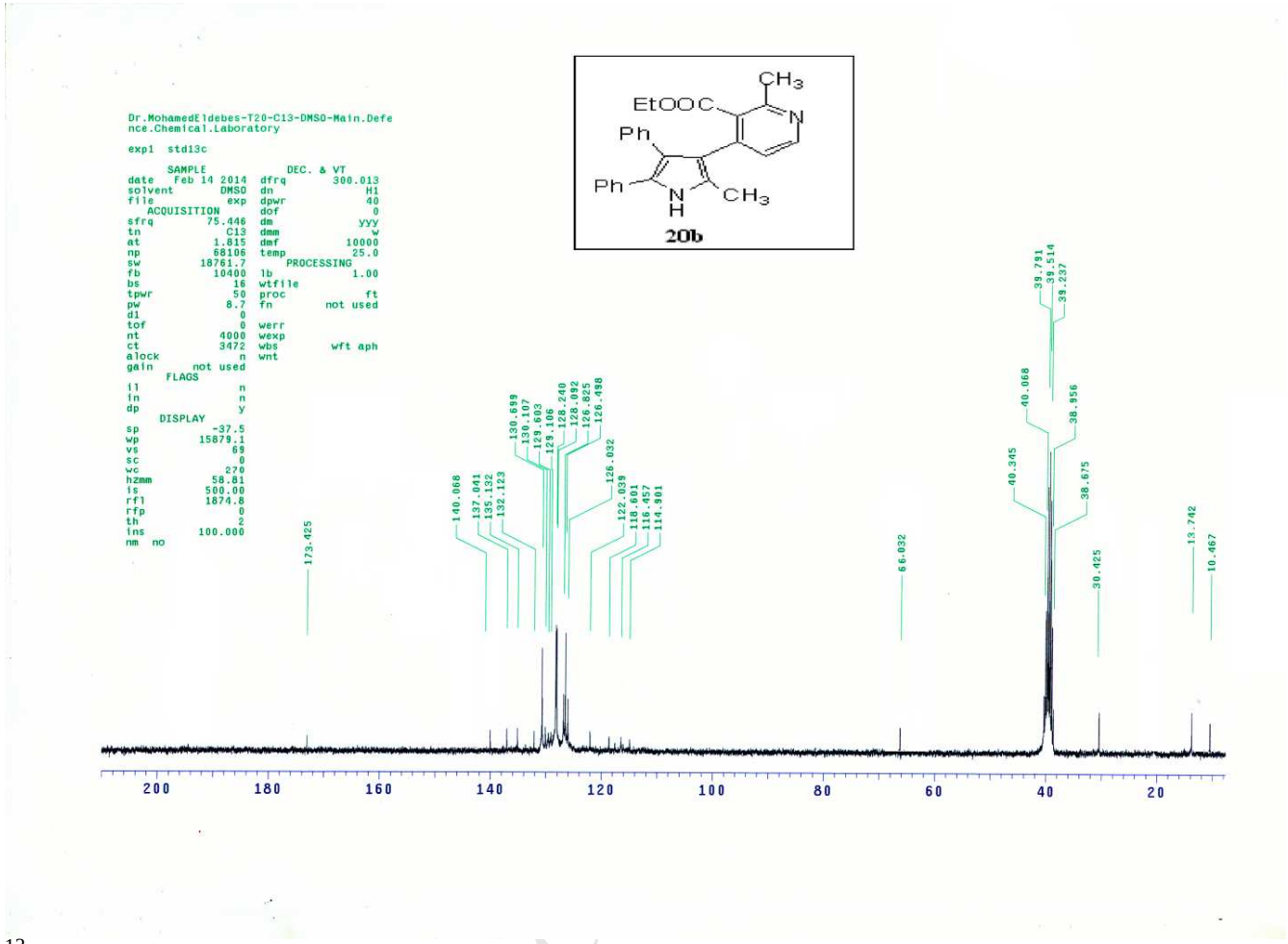

^{13}C NMR spectrum of compound **20b**

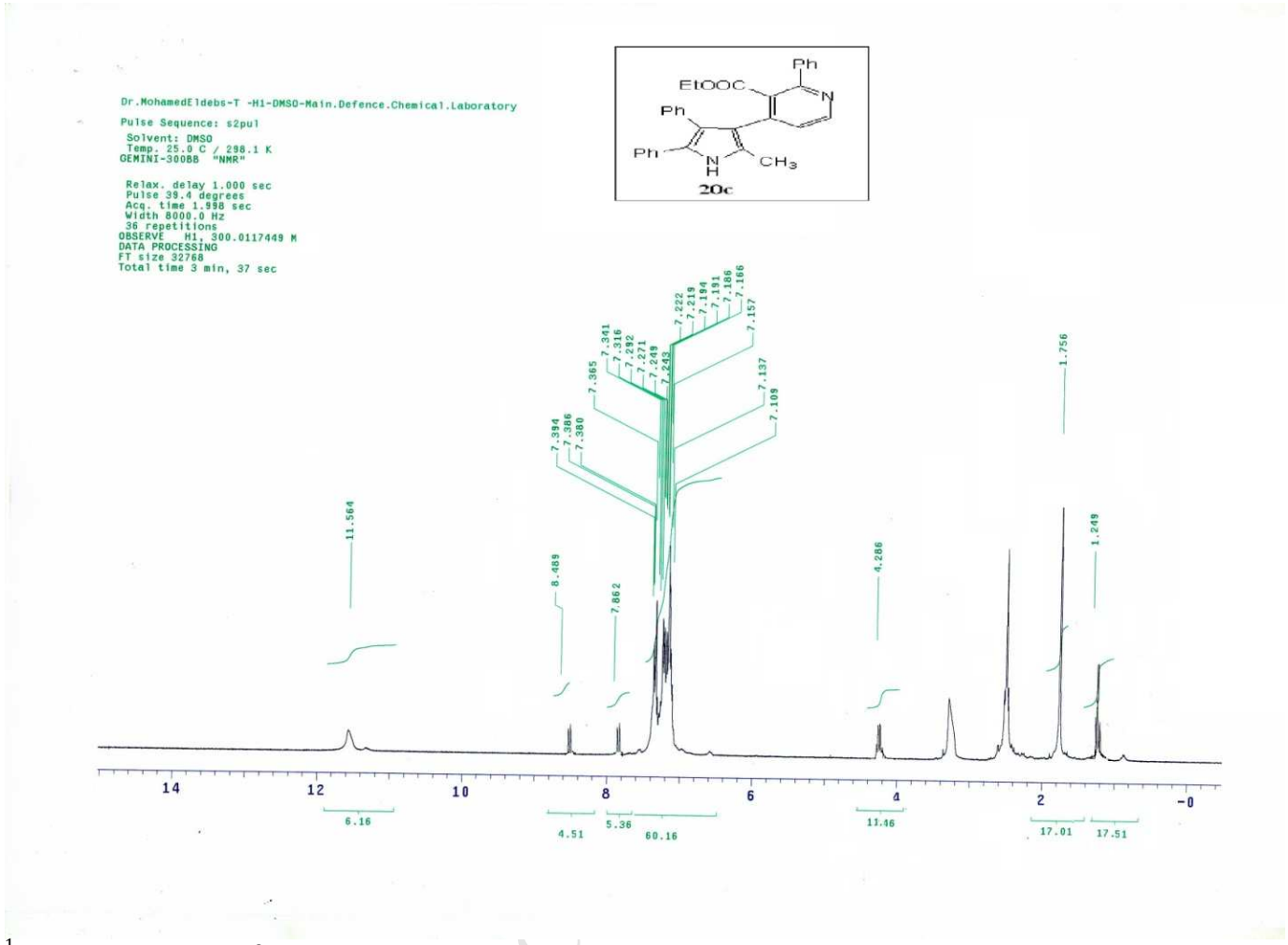

^{1}H NMR spectrum of compound **20c**

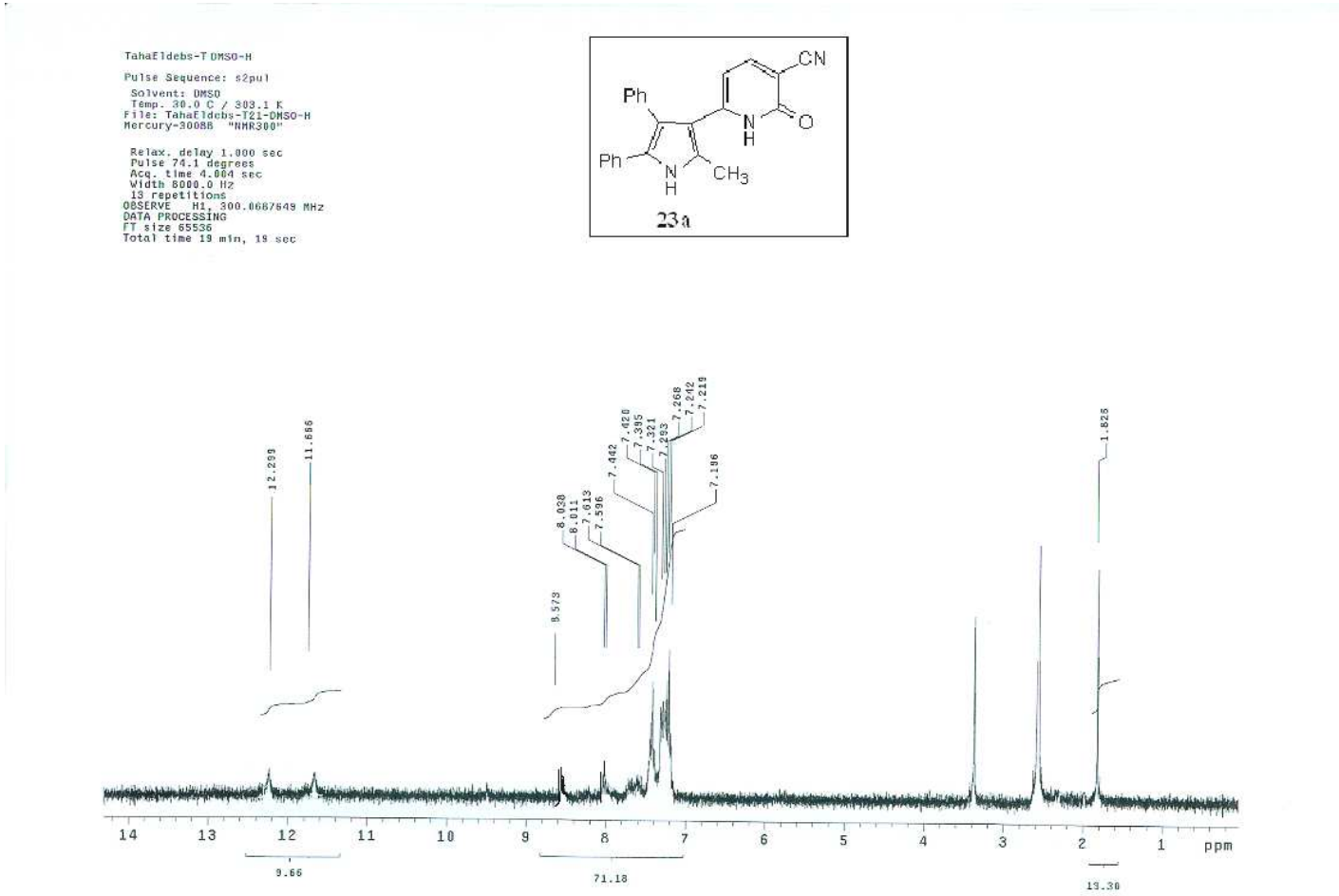

^{1}H NMR spectrum of compound **23a**